LIBRARY OF THE
UNIVERSITY OF ILLINOIS
AT URBANA-CHAMPAIGN

510.84
Il6r
no.111-130
cop.3

The person charging this material is responsible for its return to the library from which it was withdrawn on or before the **Latest Date** stamped below.

Theft, mutilation, and underlining of books are reasons for disciplinary action and may result in dismissal from the University.

To renew call Telephone Center, 333-8400

UNIVERSITY OF ILLINOIS LIBRARY AT URBANA-CHAMPAIGN

BUILDING USE ONLY

SEP 21 1980

SEP 20 1980

L161—O-1096

Digitized by the Internet Archive
in 2013

http://archive.org/details/engineeringmodel111rays

I l 6r
no. 111
cop. 3

UNIVERSITY OF ILLINOIS
GRADUATE COLLEGE
DIGITAL COMPUTER LABORATORY

This volume is bound without no.118,120-122

which is/are unavailable.

CHING

I l6r
no. 111
cop. 3

UNIVERSITY OF ILLINOIS
GRADUATE COLLEGE
DIGITAL COMPUTER LABORATORY

REPORT NO. 111

ENGINEERING MODEL OF A PARTIAL SWITCHING EFFECT IN FERRITE CORES

by

Sylvian R. Ray

September 5, 1961

UNIVERSITY OF ILLINOIS
GRADUATE COLLEGE
DIGITAL COMPUTER LABORATORY

REPORT NO. 111

ENGINEERING MODEL OF A PARTIAL SWITCHING EFFECT IN FERRITE CORES

by

Sylvian R. Ray

September 5, 1961

-130

TABLE OF CONTENTS

INTRODUCTION 1

I FUNDAMENTAL PROPERTIES OF MAGNETIC MATERIALS 3
  1 Energy Relations 3
  2 Domains and Bloch Walls 5
  3 Ferrites 6
  4 Preparation of Ferrites 7

II FLUX REVERSAL 9
  1 Engineering Model of Flux Reversal 9
  2 Rotation 10
  3 Domain Wall Motion 11
  4 Review of Menyuk and Goodenough's Contribution 12
  5 Haynes' Model 15
  6 Lindsey's Model 17

III FULL SWITCHING EQUATIONS 18
  1 Introduction 18
  2 Generalized Full Switching Equations 19
  3 Fitting Experimental Data 22
  4 Curvature of the $1/\tau_s$ versus F Curve 22
  5 Radial Effects 28
  6 Radial Models for Haynes' and Lindsey's Equations 29

IV THE MAXPEAK EFFECT 33
  1 Introduction 33
  2 Definition of the Maxpeak Effect 34
  3 Previous Investigations 36
  4 Experimental Results 37

IV THE MAXPEAK EFFECT (Continued)

5 The Formulation of a Model 39

6 The Maxpeak Effect on the Basis of Radial Effects Only 40

7 Basic Model of Maxpeak Effect 41

8 Analysis of the Basic Model 45

9 Modification of the Basic Model by Wall Velocity Distribution 50

10 Modification of Basic Model by Radial Effects 54

V THE MAXPEAK EFFECT FOR WIDER RANGE OF F_{DN} 56

1 Experimental Results 56

2 Maxpeak Effect at Low F_{DN} 58

CONCLUSION 62

1 General 62

2 Full Switching 62

3 Maxpeak Effect Model for Limited Range of F_{DN} 63

4 Maxpeak Effect Model for Wider Range of F_{DN} 65

5 Velocity Distribution 66

6 Further Work 67

APPENDIX I - EXPERIMENTAL METHOD 69

1 Drive Pulse Amplitude and Length 69

2 Waveform Measurement 71

3 Size Measurements 72

4 Core Type Used 72

APPENDIX II - RADIAL EFFECT AND MISCELLANEOUS COMPUTATIONS 73

1 General 73

2 Radial Effects 73

3 Curve Fitting 74

4 Maxpeak Effect 75

BIBLIOGRAPHY 78

VITA 79

ACKNOWLEDGEMENT

The patient guidance and many pertinent suggestions of my advisor, Professor James E. Robertson, are gratefully acknowledged. The painstaking reading and criticism of the final manuscript by Professor Kenneth C. Smith was greatly appreciated.

Sincere thanks are also extended to Mr. John L. Fileccia for his relentless aid with the lengthy computer calculations, and to Mrs. Helen Peek and Mrs. Marilyn Briley who typed the final copy.

INTRODUCTION

The widespread use of square hysteresis loop ferrite materials in computer technology has directed attention to the problem of constructing an engineering model of the process of flux reversal. Such a model would, ideally, allow the square loop ferrite specimen to be treated, in circuit design, as any other common circuit component. For the simplest geometry, the toroid, the problem is just to establish the voltage-current relation for a two-terminal network, the terminals being the two ends of a conductor which links the magnetic flux of the toroid.

Notable success has been achieved by previous investigators. A broad area of theoretical and experimental work was effectively coordinated by Menyuk and Goodenough (1955) resulting in basic equations of the process of flux reversal by domain-wall motion and clarifying certain questions of the related microscopic details. First, Haynes (1958) and, later, Lindsey (1959) specified the function, $F(<r>)$, which remained in the Menyuk-Goodenough equations, resulting in practical equations of flux reversal.

The simplest experiment producing flux reversal in a magnetic core consists of the application of a step function of mmf with the core initially in one of its two reproducible (saturated) states. Even for this experiment, the known models are demonstrably inaccurate, although adequate for some applications. It will be shown presently that this problem may be resolved by generalizing the models of Lindsey and Haynes.

The more interesting problem which is investigated here is that of construction of a model for "partial switching", that is, the case of flux reversal proceeding from an initially unsaturated state. Attention is focused on a particular type of partial switching, that in which the intermediate state is reached by a pulse of mmf in the "UP" (set) direction.

The response to a pulse in the "DOWN" (reset) direction is then examined. Certain invariant and semi-invariant quantities are found to exist for the observed response. In particular, the envelope of peak amplitudes of the voltage versus time curves itself reaches a maximum, the "maxpeak", which appears at first sight to be anomalously large. It is demonstrated that a logical extension of Lindsey's model is adequate to explain the observations in a rudimentary way. In addition, the study of the maxpeak effect model is believed to provide a more stringent test of some of the assumptions of the earlier models.

In the construction of flux reversal models, the principal constraint in the present work is that the model be based on microscopic switching processes which are physically rational. Stated negatively, purely mathematical models are not considered.

I. FUNDAMENTAL PROPERTIES OF MAGNETIC MATERIALS

I.1 Energy Relations

In order to proceed with the discussion of magnetic effects, it is desirable to review, however briefly, the kinds of energy upon which these effects depend. This has been done by Van Vleck (1956), whose classification is followed here.

(1) Zeeman Energy

This is the energy which exists in the interaction of the applied magnetic field, $\vec{H}_i$, with electron spin and orbital angular momenta which can be written

$$E_z = -g\beta \sum_i (\vec{H} \cdot \vec{S}_i) \qquad (1.1)$$

where g is the spectroscopic splitting factor (≈ 2)

β is the Bohr magneton

$\vec{S}_i$ is the spin angular momentum of the i^{th} electron.

Since the electrons tend to occur in antiparallel pairs in conformance with the exclusion principle, only a very small percentage of electrons in a material absorb net energy from the applied field. The substantial magnetic effects in Fe, Ni, and Co are due to the unusually large number (up to 5) of unpaired electron spins.

(2) Classical Electromagnetic Dipolar Energy

This is the energy effect commonly observed, on macroscopic level, as the tendency of bar magnets to align themselves such that the direction of maximum length corresponds to the direction of the magnetization vector. At atomic distances, the dipolar energy is masked by other

interactions. Its long range effect, however, accounts for the appearance of domain structure.

(3) Exchange Energy

The exchange energy is most simply expressed by the relation

$$E_x \cong -2J \sum_{i \leftrightarrow j} \vec{S}_i \cdot \vec{S}_j \tag{1.2}$$

where J is the quantum mechanical exchange integral and $i \leftrightarrow j$ implies summation over nearest neighboring atoms. This energy accounts for a large portion of the short-range ordering of spins which, it should be noted, is a prime requisite to establishing magnetic effects. It can also be seen that exchange energy is independent of external direction references, i.e., it depends solely upon the relative spin directions and magnitudes.

(4) Anisotropic Exchange Energy

This energy results from the interaction of spin with spherically asymmetric orbital charge distribution. This effect is similar to the classical dipolar energy except that anisotropic exchange is sufficiently stronger at small distances to account for the powerful anisotropic effects observed in solids. The anisotropy energy has the macroscopic form:

$$E_A \cong A\alpha_1^2 + B\alpha_2^2 + C\alpha_3^2 \tag{1.3}$$

where A, B, and C are constants and α_1, α_2, and α_3 are the direction cosines of the angles between the direction of magnetization and the principal crystal axes.

A sketchy physical conception of the origin of magnetic effects may be extracted from the more formal statements above. In a magnetic specimen, the crystal structure determines the favorable orbital electron motion. The orbital motion affects, by anisotropic exchange, the spin direction. In ferromagnetic materials, a substantial net spin may

Loaded
for Deck
1
9/30/80
TL

ls

nite, single crystal of a magnetic material, it
gnetization exists which would necessarily
through the surrounding medium, e.g., air.
energy required to establish the flux in a
is preferable to close the field within the
be done, for example, as illustrated in Fig. 1.1
on vectors are indicated. In other terms,
on (demagnetization component) due to the
ior by the long-range dipolar mechanism.
iform magnetization are domains or, "Weiss
ween domains is a Bloch wall (domain wall)
xplained in the following paragraph.

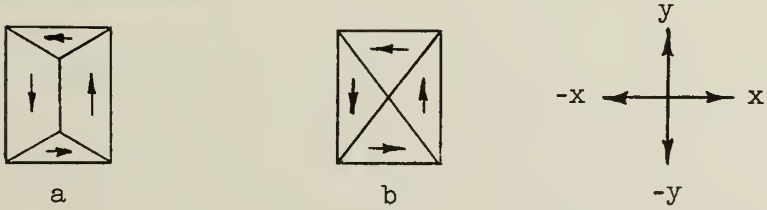

a

b

Figure 1.1

A sketchy physical conception of the origin of magnetic effects may be extracted from the more formal statements above. In a magnetic specimen, the crystal structure determines the favorable orbital electron motion. The orbital motion affects, by anisotropic exchange, the spin direction. In ferromagnetic materials, a substantial net spin may result.

I.2 Domains and Bloch Walls

In a perfect, finite, single crystal of a magnetic material, it might appear that a net magnetization exists which would necessarily generate return flux paths through the surrounding medium, e.g., air. Due to the relatively large energy required to establish the flux in a low permeability medium, it is preferable to close the field within the magnetic medium. This can be done, for example, as illustrated in Fig. 1.1 a, b where the magnetization vectors are indicated. In other terms, the surface pole distribution (demagnetization component) due to the boundary, affects the interior by the long-range dipolar mechanism. The resulting regions of uniform magnetization are domains or, "Weiss domains". The boundary between domains is a Bloch wall (domain wall) whose characteristics are explained in the following paragraph.

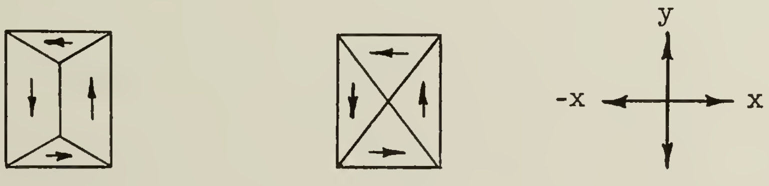

a b

Figure 1.1

If the maximum space rate of change of the direction of magnetization in the Bloch wall is very great, it can be seen from equation (1.2) that the exchange energy would be large ($J > 0$ assumed) so that this energy favors a wide Bloch wall with negligible magnetization change from one atom to the next. However, assuming only the $\pm x$ and $\pm y$ directions of Fig. 1.1 correspond to low anisotropy energy, the slow change of magnetization in the Bloch wall would compel large numbers of atomic magnetization vectors into directions of high anistropy energy. Thus a compromise arises which results in Bloch walls having small but non-negligible widths (of the order of 100 Å).

The change in angle of the magnetization vector from one domain to another contiguous domain is used to classify domain walls. In Fig. 1.1 a, for example, there are four 90° and one 180° domain walls.

The characteristics of domains will be relegated to section II.1.

I.3 Ferrites

The ferrites are metallic oxides whose molecular formula is $XO \cdot Y_2O_3$ where X corresponds to a metallic atom of valence 2 and Y corresponds to a metallic atom of valence 3.

A wide variety of metals may be employed, the iron group being particularly common. The oxygen atoms provide bonds for the metallic electrons which would otherwise be free for electrical conduction. Thus, the electrical conductivity of ferrites may be very low. This fact is of engineering importance in two ways. First, the eddy current losses which characterize other magnetic materials are eliminated. Secondly, the maximum rate of change of magnetization, which would otherwise be limited by the eddy current field, may be very great. The second factor is particularly desirable in computer technology.

In ferromagnetic materials, all unpaired electron spins within a unit cell of the material are approximately aligned so that all contribute

to the magnetization. In ferromagnetic materials, (i.e., ferrites), certain electron spins which are unpaired within their own atom, may cancel the magnetic contribution of similar electrons in neighboring atoms. If the cancellation within a unit cell is total, the material is said to be antiferromagnetic. If the cancellation is only partial, the material displays ordinary ferrimagnetism.

The metallic atoms which can contribute to the magnetization in ferrites may occupy two types of sites, called A and B sites. In a unit cell of ferrite, the number of such sites occur in the ratio 1:2. If the exchange energy between B sites is large, a degree of antiparallel alignment of B atoms results. Thus, the attendant magnetic contribution of the B sites is small. This structure is called "normal". If the B atomic spins are aligned but antiparallel to the spin of A atoms, the structure is said to be of the "inverse" type.

I.4 Preparation of Ferrites

The ferrite bodies which are of interest here have polycrystalline structure and are prepared by the following procedure. A mixture of metallic oxides is powdered by a ball-milling process; the resulting mixture, including possibly a binder material, is packed into a mould and the desired hole(s) punched out. The body is then sintered for periods of one minute to several hours at temperatures of approximately 1300°C in the presence of a gaseous atmosphere, such as nitrogen. The various parameters must, in general, be rigidly controlled in order to obtain adequately reproducible results.

It should be noted that no magnetic orientation (annealing) is employed so that the bodies are magnetically isotropic barring possible shape effects.

As a result of its method of fabrication, a ferrite body usually contains a number of voids (typically 10% of the volume) whose distribution in shape, size, and position appears to be quite random. The crystal structure is further disarrayed by grain boundaries which leave a random distribution of volumes having a periodic crystal structure.

Photomicrograms of the cross-section of ferrite bodies are found in Smit and Wijn (1959).

II. FLUX REVERSAL

II.1 Engineering Model of Flux Reversal

In order to precisely design electrical circuits using a toroidal magnetic core, it is only necessary, theoretically, to know the current-voltage relation for a single wire linking the toroidal path for all possible (time-varying) currents through the wire. From the viewpoint of practical engineering design, such a relation would probably be too cumbersome for general use. It would, however, be desirable to have a mathematical model of flux switching in these cores which is reasonably accurate over a wide range of conditions, even at the expense of being too cumbersome for usual design work. The mathematical model would then have the possibility of being simplified for special cases.

Previous efforts to formulate such models have been based on the assumption that the magnetic specimen is initially in a saturated state. Such equations are of the form:

$$\dot{M} = f(M,H)$$

with $\dot{M}$ = the time rate of change of magnetization

M = the magnetization, and

H = the applied field intensity.

This equation can also be written

$$\dot{\phi} = f(\phi, H)$$

to a negligible approximation in most cases since the induction directly contributed by H, ($\mu_o H$), is very small compared to M in the relation

$$B = \mu_o H + M.$$

Only at times when $\dot{H}$ is large is there any practical concern in replacing $\dot{M}$ by $\dot{\phi}$.

The circularly directed component of magnetization is the only component of interest here; hence, scalar notation is employed.

The equations of the previous type which have been derived are based on switching by (a) 180° domain-wall motion, (b) rotation. The equation for rotation was derived by Gyorgy (1957) from the Landau-Lifshitz phenomenological damping equation. The present investigation will be limited to the domain-wall motion model formulated by Menyuk and Goodenough (1955) and extended by Haynes (1958) and Lindsey (1959).

II.2 Rotation

Flux changes may occur by rotation as a result of the interaction of the magnetic field intensity, $\vec{H}$, with the magnetization, $\vec{M}$. The resulting torque, causing rotation, is $\vec{T} = \vec{M} \times \vec{H}$.

If the field, H, is small, only individual atomic spins are rotated against the anisotropic exchange force and the action is generally characterized by small, fast ($\approx$ 1 mμs) reversible changes of magnetization. If, however, sufficiently large fields are applied, the magnetization of a complete domain or sample of material may be moved past the direction of maximum anisotropic or demagnetizing force such that, upon removal of the applied field, a different arrangement of domains exists, i.e., the flux change is now irreversible. At some intermediate field, it is possible, according to Gyorgy (1958), to rotate the magnetization in such a way that the demagnetizing effects may be neglected. If the magnetization of the whole volume of material in question is irreversibly changed by rotation against demagnetizing forces, the switching process is said to be coherent or uniform rotational switching.

If the magnetization is rotated in a way such that the demagnetizing effects may be neglected, the switching process is then incoherent or nonuniform rotation.

Estimates by Smith (1960) indicate that the minimum drive for which rotational effects can occur is four times the threshold field for materials similar to the ones used in the present study. The present investigation will be carried out for fields smaller than the rotation threshold.

II.3 Domain Wall Motion

The voids, grain boundaries, and other imperfections in a polycrystalline ferrite have a fundamental effect on the magnetic properties of the material. It can readily be seen that voids of sufficient size are analogous to the boundary of the material, thereby causing the formation of 90° domain walls (closure domains) and surface poles as explained in section I.2.

The process of flux reversal by domain wall motion is generally pictured as follows: starting from an initial condition of spontaneous magnetization, a sufficiently large magnetic field applied in the reverse direction causes a 180° Bloch wall to be initiated or "nucleated" along a grain boundary. As the Bloch wall moves, the volume in its wake is left with the magnetization reversed. The wall continues to move until either (1) it meets another wall moving toward it, which annihilates both, or (2) the driving field is removed, in which case the wall comes to rest in a way consistent with requirements of minimum potential energy.

As a domain of reverse magnetization grows due to the pressure of the applied magnetic field, the increasing domain wall surface area absorbs energy from the driving field. In high resistivity material, this energy is lost to damping effects which arise from the delayed response of atomic spins

to the force which tends to change their direction. It is usually assumed that this damping is viscous so that domain walls subjected to a steady field will move with constant velocity, once the initial acceleration has been completed.

The conditions which must be met in order to attain squareness of the hysteresis loop are also of interest. According to Goodenough (1954), the nucleation of a domain wall occurs when the energy required to form surface poles at the grain boundary becomes larger than the energy required to form a region of reverse magnetization. Therefore, at applied field intensities below the nucleation threshold, the formation of surface poles must be preferred. This is expressed by Goodenough's result,

$$LM_s^2(\cos \theta_1 - \cos \theta_2)^2 < 60\,\sigma_w$$

where L is the mean grain diameter

M_s is the spontaneous magnetization

θ_1, θ_2 are the directions of magnetization in adjacent grains relative to their common boundary and

σ_w is the surface energy density of a 180° Bloch wall.

The above condition is believed to be met in magnetically annealed materials because of the small value of $(\cos \theta_1 - \cos \theta_2)^2$ while in polycrystalline ferrites, it is due to the small value of M_s^2.

II.4 Review of Menyuk and Goodenough's Contribution

A major step toward the development of a model of flux switching was taken by Menyuk and Goodenough (1955). They consider the expanding domains to be ellipsoids having large semimajor to semiminor axis ratio and derive the relation

$$\beta \frac{d\langle r\rangle}{dt} = 2I_s(H_m - H_o)\langle\cos \theta\rangle \tag{2.1}$$

where β is the damping parameter

$\langle r \rangle$ is the mean value of semiminor axis at the center of the domain

I_s is the spontaneous magnetization

H_m is the applied field intensity

H_o is the threshold field, that is, the upper bound of field intensity for which the domain wall velocity is zero, and

θ is the angle between the domain's magnetization vector and the applied magnetic field direction.

It should be noted that the preceding equation is based on the assumption that the domain walls move with constant velocity, that is, $H_m - H_o = \text{constant} > 0$. Integration of (2.1) yields the now-classic relation for H_m independent of time:

$$(H_m - H_o)\tau_s = S_w \tag{2.2}$$

where τ_s is the switching time and

S_w is the switching coefficient, a constant which depends on the properties of the core material.

They proceed further to write the time rate of change of irreversible flux, formally, as

$$\frac{d\phi}{dt}_{irr} \propto F(\langle r \rangle)(H_m - H_o) \tag{2.3}$$

where $F(\langle r \rangle) = \frac{\partial A_c}{\partial \langle r \rangle}$, A_c being the cross-sectional area of the core in which flux has been reversed.

A typical example of a full switching curve is given in Fig. 2.1.

A direct quotation from the Menyuk-Goodenough paper will serve to elucidate their view of the flux reversal process.

> "$F(\langle r \rangle)$ measures the rate of change of flux as a function of the constant-velocity-wall positions. Since the average wall velocity is assumed to accelerate to a constant velocity in a

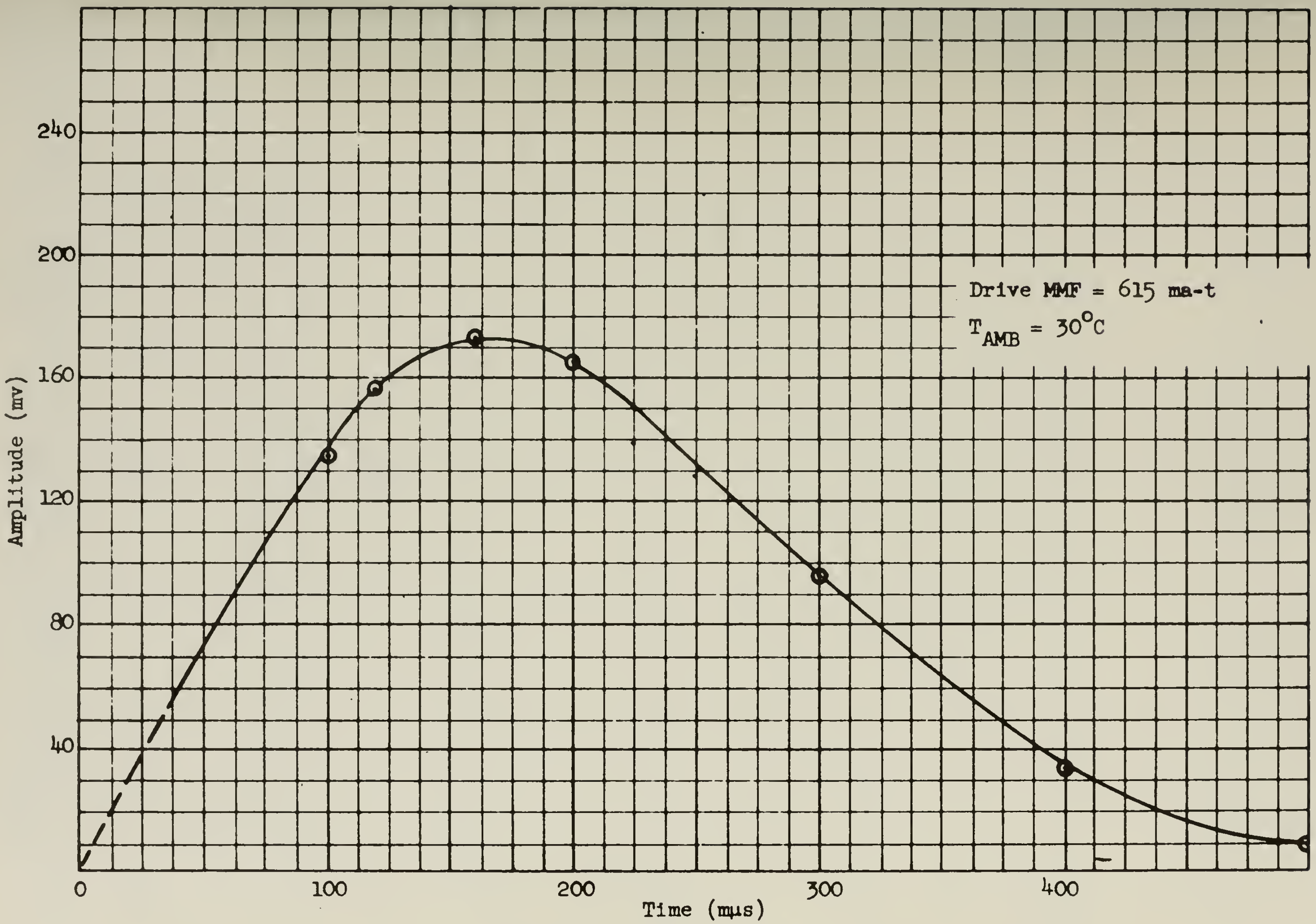

Figure 2.1 Experimental Full Switching Curve

> time t << τ, F(<r>) is a maximum when the wall area encompassing the growing domains is a maximum. The wall area surrounding a growing domain increases with r until it collides with similarly growing domains and is annihilated. Because of the ramdom distribution of the growing domains throughout the specimen, at larger values of r, F(<r>) decreases to zero with a Gaussian-like tail."

II.5 Haynes' Model

Haynes (1958), proceeding from the previously described development of Menyuk and Goodenough, introduced assumptions required to specify the function, F(<r>). Haynes states the following explicit assumptions:

(1) Only irreversible wall motion is treated.

(2) The nucleation field strength is equal to the threshold field.

(3) The number of nucleated domains is independent of $H - H_o$.

(4) The nucleation process and the finite minimum size of a domain are neglected.

(5) The variation of H with radial position with a core is neglected.

(6) $\partial A_c / \partial \langle s \rangle$ is a function of domain wall position, <s>, and not of the velocity d<s>/dt.[1]

Haynes makes the further assumption that the distribution of nucleating centers throughout the core volume is specified by a Poisson distribution. Thus,

$$P(n,V) = \frac{(qV)^n}{n!} e^{-qV} \qquad (2.4)$$

is the probability of exactly n nucleating centers occurring in a volume, V, where q is the expected number of nucleating centers per unit volume. A number, k, is then defined so that

$$qV = k^3 s^3 \qquad (2.5)$$

---

[1] Haynes' <s> is equivalent to Menyuk and Goodenough's <r>. All of these assumptions except (4) and (5) are explicitly or implicitly contained in the equations of Menyuk and Goodenough which are employed in the subsequent development.

where s is the length of the semi-minor axis of an ellipsoidal domain measured at the center. Haynes then proceeds to compute the rate at which core cross-sectional area is added to the new direction of magnetization. Substituting the expression for this rate into the equations of Menyuk and Goodenough, there is obtained the result

$$\Phi = \langle\cos\Theta\rangle \Phi_s (1 - 2e^{-qV}) \qquad (2.6)$$

where the initial condition

$$\Phi_o = -\langle\cos\Theta\rangle \Phi_s \qquad (2.7)$$

has been included. In the above expressions

Φ is the magnetic flux and

Φ_s is the spontaneous or remanent value of flux.

Normalizing the flux by defining

$$x \equiv \frac{\Phi}{\Phi_s \langle\cos\Theta\rangle} \qquad (2.8)$$

and using relation (2.5),

$$x = 1 - 2e^{-k^3\langle s\rangle^3} \qquad (2.9)$$

which can be differentiated and combined with equations (2.1) and (2.3) to give:

$$\frac{dx}{dt} = \frac{6kI_s}{\beta} \langle\cos\Theta\rangle (H - H_o)(1 - x)\left(-\ln\frac{1 - x}{2}\right)^{2/3}. \qquad (2.10)$$

It should be noted here that x lies in the range (-1, 1) with x = -1 (as implied by equation (2.7)) as the initial value.

Equation (2.10) can be written in terms of experimentally determinable constants by considering the solutions of (2.10) when H is independent of time, i.e., a step function. The family of curves, dx(t)/dt for the parameter, H,

exhibits a distinct peak value and peaking time which allows k and <s> to be related to S_w as defined in equation (2.2). Haynes' final result is:

$$\frac{dx}{dt} = \frac{4.82}{S_w}(H - H_o)(1 - x)(-\ln\frac{1 - x}{2})^{2/3} . \tag{2.11}$$

This equation will be considered in detail in the next chapter.

II.6 Lindsey's Model

Lindsey (1959), starting from the Menyuk-Goodenough results, also developed an equation for the function F(<r>)(see equation (2.3)). The only basic difference between Lindsey's and Haynes' development is that Lindsey considers the flux reversal to be accomplished by expanding cylindrical rather than elongated ellipsoidal domains. Lindsey finds that the core output voltage for constant applied driving field is given by:

$$\frac{d\phi}{dt} = k_1 H_e^2 t \, e^{-k_2 H_e^2 t^2} \tag{2.12}$$

whereas the equivalent form of Haynes' result, as will subsequently be shown, is:

$$\frac{d\phi}{dt} = k_3 H_e^3 t^2 e^{-k_4 H_e^3 t^3} . \tag{2.13}$$

These results will be compared in the next chapter.

III. FULL SWITCHING EQUATIONS

III.1 Introduction

In order to provide a basis for extension of a model of switching into the partial switching mode, it is desirable to determine which model of full switching most closely corresponds to reality. This is done in the present investigation by generalizing the results of Haynes and Lindsey and examining the ensuing family of equations.

The generalized full-switching equation is shown to have certain mathematically-desirable properties: first, the product of peaking time, t_p, and normalized peak amplitude, $\dot{x}_p$, is independent of driving field, threshold field, and switching constant; second, the experimentally-found curvature of the reciprocal switching time curve can be duplicated by varying a single parameter, n; third, any usual definitions of switching time are also shown to be directly proportional to one another, in an easily calculated way, for any member of the equation family.[1]

On the latter point, it should be noted that many definitions of switching time have been employed. For example, the time during which the switching waveform amplitude exceeds 10% of its peak amplitude was used by Menyuk and Goodenough (1955). The time for 90% of flux switching has also been used, e.g., by Shevel (1958).

It is also shown that within the family of equations considered, the introduction of radial effects (integration of the curves over radius) does not lead to the curvature of the inverse switching time curve which is experimentally observed.

---

[1] Haynes pointed this out, essentially, for his equation ($n = 3$).

III.2 Generalized Full Switching Equations

Haynes' equation is analytically soluble for H independent of t, i.e., for a step function of applied driving field. Under this condition and for $H - H_o > 0$, it is found that:

$$x = 1 - 2 \exp[-(Kt)^3] \tag{3.1}$$

$$\dot{x} = 6K^3t^2 \exp[-(Kt)^3] \tag{3.2}$$

where $K = \frac{4.82}{3} \frac{H - H_o}{S_w}$

$x = \frac{\phi}{\phi_s}$ where $\phi_s = \Phi_s \langle\cos \Theta\rangle$, the observed remanent flux

$\dot{x} = \frac{dx}{dt}$

H = the net applied field intensity

H_o = the threshold field

S_w = the switching constant, and

t = time.

It has been assumed here that $x = -1$ for $t = 0$ and that x has the range $[-1, 1]$. Note that $H - H_o > 0$ must hold for the meaningful application of the equations.

We shall now consider a family of equations of which (3.1) is a member, namely,

$$x_n = 1 - 2 \exp[-(Kt)^n] \tag{3.3}$$

$n > 1$ being the region of interest. Then differentiating (3.3) with respect to t,

$$\dot{x}_n = 2nK^nt^{n-1} \exp[-(Kt)^n] \; . \tag{3.4}$$

The time, t_{np}, at which the maximum value of (3.4) occurs is given by the solution of:

$$\ddot{x}_n = 0 = 2nK^n \left\{ t_{np}^{n-1}[-nK^n t_{np}^{n-1}] + (n - 1)t_{np}^{n-2} \right\} \exp\left\{ -[Kt_{np}]^n \right\} .$$

$$\therefore \qquad -nK^n t_{np}^n + (n - 1) = 0$$

$$t_{np} = \frac{\left(\frac{n - 1}{n}\right)^{1/n}}{K} . \qquad (3.5)$$

Substituting (3.5) into (3.4), and setting $\dot{x}_n(t_{np}) = \dot{x}_{np}$,

$$\dot{x}_{np} = 2nK^n \frac{\left(\frac{n - 1}{n}\right)^{(n-1)/n}}{K^{n-1}} \exp\left\{- \frac{n - 1}{n}\right\}$$

$$\dot{x}_{np} = 2n \left(\frac{n - 1}{n}\right)^{(n-1)/n} e^{-\frac{n-1}{n}} K . \qquad (3.6)$$

Multiplying (3.5) by (3.6), we obtain

$$t_{np}\dot{x}_{np} = 2n \left(\frac{n - 1}{n}\right) e^{-\frac{n-1}{n}}$$

$$t_{np}\dot{x}_{np} = 2(n - 1)\, e^{-\frac{n-1}{n}} . \qquad (3.7)$$

Hence, we have the conclusion that $\dot{x}_{np}t_{np}$ is dependent only on n, being independent of K, regardless of the possible dependency of K on n.

Also, the value $x(t_p) = x_p$ is independent of K, which can easily be seen by substituting (3.5) into (3.3), whereupon:

$$x_p = 1 - 2e^{-\frac{n-1}{n}} . \qquad (3.8)$$

It can also be shown that any given fraction, α, of the peak time rate of flux change, $\dot{x}_{np}$, occurs at a time which is a constant multiple, β, of the peaking time, independent of the value of K. Thus, using (3.4),

$$\dot{x}_n = \alpha\dot{x}_{np} = 2nK^n t^{n-1} e^{-[Kt]^n}$$

and setting $t = \beta t_{np}$ where $0 \leq \alpha \leq 1$ and $\beta \geq 0$

$$\alpha\dot{x}_{np} = 2nK^n \beta^{n-1} t_{np}^{n-1} e^{-[K\beta t_{np}]^n} \quad .$$

Substituting (3.5) and (3.6),

$$\alpha \cdot 2n \left(\frac{n-1}{n}\right)^{(n-1)/n} e^{-\frac{n-1}{n}} K = 2n\beta^{n-1} K \left(\frac{n-1}{n}\right)^{(n-1)/n} e^{-\beta^n\left(\frac{n-1}{n}\right)}$$

$$\alpha = \beta^{n-1} e^{\frac{n-1}{n}(1-\beta^n)} \tag{3.9}$$

which establishes the preceding statement. Two solutions, β_1 and β_2, one before and one after peak amplitude, exist for each $0 < \alpha < 1$ for a given n.

Any given value of x can also be related to a constant (relative to K) by substituting $t = \beta t_p$ into (3.3), from which:

$$x = 1 - 2e^{-\frac{n-1}{n}\beta^n} \quad . \tag{3.10}$$

Therefore, for any member of the family of equations, i.e., for any $n > 1$, the relation of x or of any fraction of $\dot{x}_p$ to the peaking time is constant. Hence, all usual definitions of switching time, whether given by the time to some value of x or some fraction of $\dot{x}_p$, are conveniently interrelated within this family. Similary, the ratio of switching time to peaking time is a constant for any n. The meaning of non-integer n is

problematical and will be discussed in a more appropriate context (Chapter V).

III.3 Fitting Experimental Data

Table 1 and Fig. 3.1 present a typical group of experimental values of $\dot{x}_p t_p$ (the peak amplitude-time product), which are observed for full switching, i.e., for a saturated state as the initial condition of the core. The value of $\dot{x}_p t_p$ is, clearly, a monotonically increasing[1] function of F, the applied mmf. Since the experimental value of $\dot{x}_p t_p$ is not constant, the model of full switching, which predicts constant $\dot{x}_p t_p$, is limited in accuracy, for any single n in equation (3.3), at the outset. It should be noted that since equation (3.7) is independent of K, it is impossible to contrive a function, $K(H, H_o, S_w)$ which conforms to experiment over a range of H (with n constant and H, H_o, and S_w independent of time). Therefore, both Haynes' and Lindsey's models (which are members of the class of equations being studied) are faulty to some degree.

Equation (3.7) is plotted as Fig. 3.2. The values of n which correspond most closely to the various experimental values of $\dot{x}_p t_p$ may be conveniently found from Fig. 3.2. The values so obtained vary from about 1.8 to 2.2 for the range of applied drives listed in Table 1, which is the range of interest for later work. Hence, the vicinity of Lindsey's equation (n = 2) corresponds, on this basis, to the more nearly correct model.

III.4 Curvature of the $1/\tau_s$ versus F Curve

One of the basic relations of the Menyuk-Goodenough (1955) model is, for step functions of H and assuming initial saturation,

---

[1] One case does not conform, this being attributed to "experimental error".

Table 1

F (ma.-t.)	$\dot{\phi}_p$ (mv.)	$\dot{x}_p = \frac{\dot{\phi}_p}{\phi_s}$ $(\mu s.)^{-1}$	t_p (µs.)	$\dot{x}_p t_p$
450	71.5	3.03	0.29	0.878
500	94.5	4.00	0.24	0.96
550	123	5.22	0.19	0.992
600	150	6.36	0.17	1.082
650	178	7.54	0.14	1.057
700	208	8.82	0.13	1.148
750	240	10.17	0.118	1.198
800	274	11.60	0.105	1.218
850	308	13.03	0.095	1.238

$$\phi_s = 23.6 \cdot 10^{-9} \text{ webers}$$

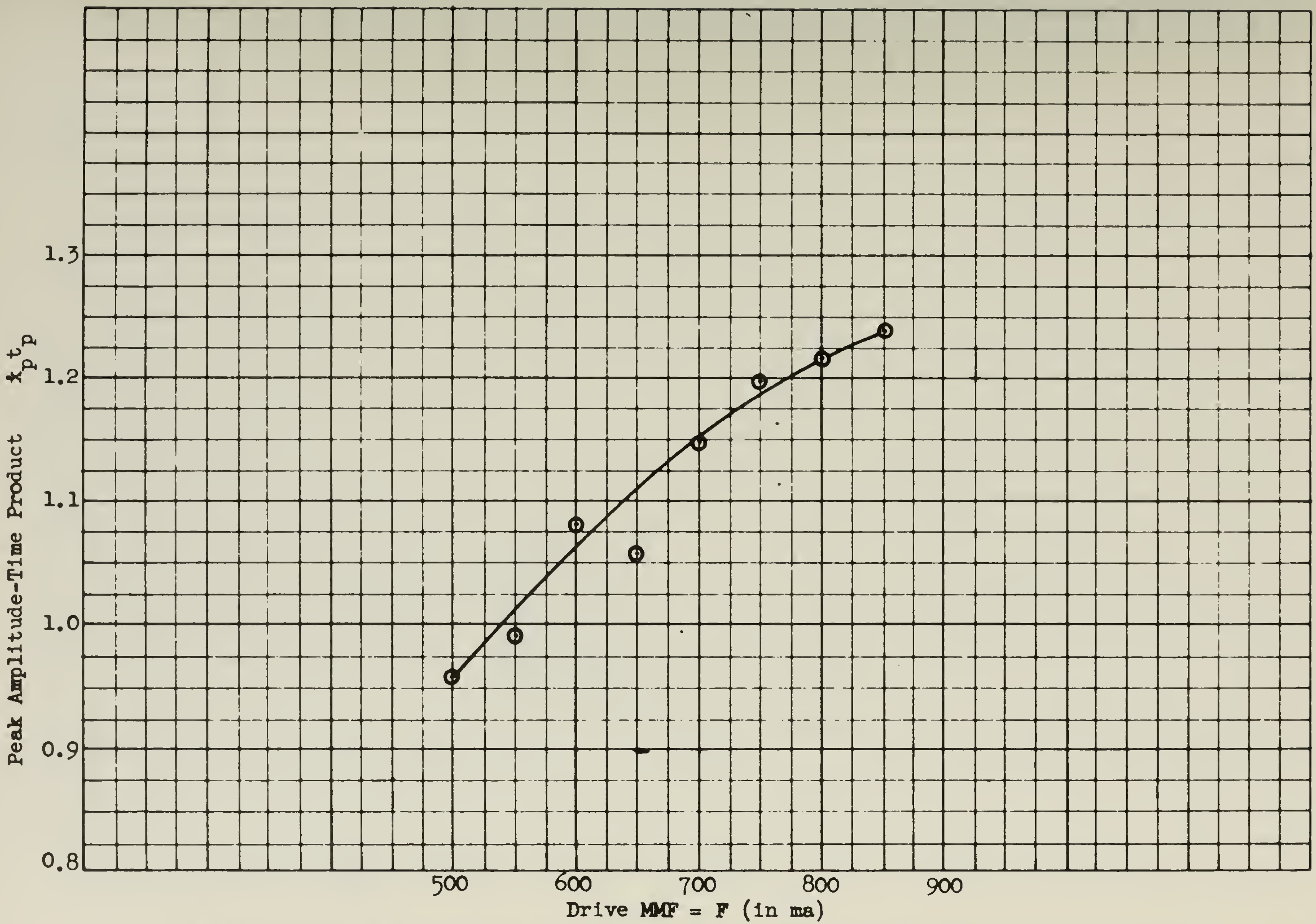

Figure 3.1 Experimental Values of the Peak Amplitude-Time Product (Full Switching)

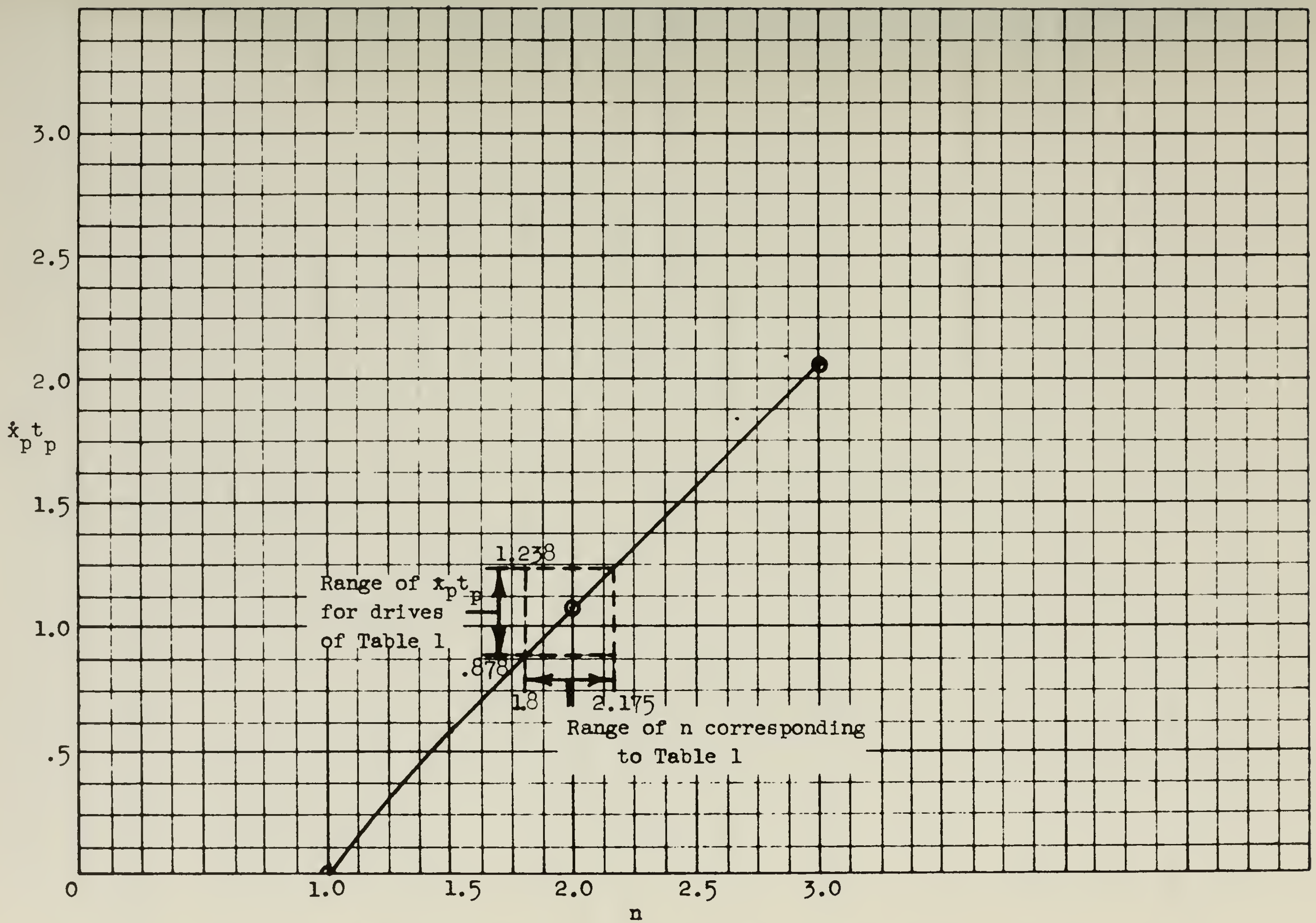

Figure 3.2 $\dot{x}_p t_p$ versus n as Derived from Generalized Full-Switching Equation

$$(H - H_o) \frac{1}{\tau_s} = S_w$$

where τ_s is the switching time and is defined as the interval between the points of 10% peak amplitude (of the irreversible component).

This relation was inferred from experiment and is often presented as a linear relation between $1/\tau_s$ and F, the applied mmf. It should also be noted that if the abscissa of such a curve is labelled in units of field intensity, this is always obtained by some relation of the form

$$H = \frac{F}{\ell_m}$$

ℓ_m being the mean path length through the magnetic specimen. This curve is usually called the "inverse switching time" curve.

It was found experimentally by Gyorgy (1957) and later verified by many investigators using fast rise-time drive pulses, that the inverse switching time curve is concave upward. Gyorgy used a different definition of switching time (viz., the time from 10% to 90% of flux change) than most earlier investigators, but there is no reason to doubt that his definition differs by other than a constant from the earlier definition.

Fig. 3.3 is a graph of v_p (the peak amplitude of the irreversible flux change) plotted against drive mmf, F. It is also concave upward, which reflects the fact that since $1/\tau_s$ (or $1/t_p$) is increasing faster than linearly and the area under the switching waveforms is constant, the peak amplitude is likely to rise at a faster-than-linear rate. This effect is also seen in the increasing values of $\dot{x}_p t_p$ in Table 1.

It is therefore not surprising that neither Haynes' nor Lindsey's equation exactly fits experimental observations, since both are based on the linear reciprocal switching time relation through the Menyuk-Goodenough

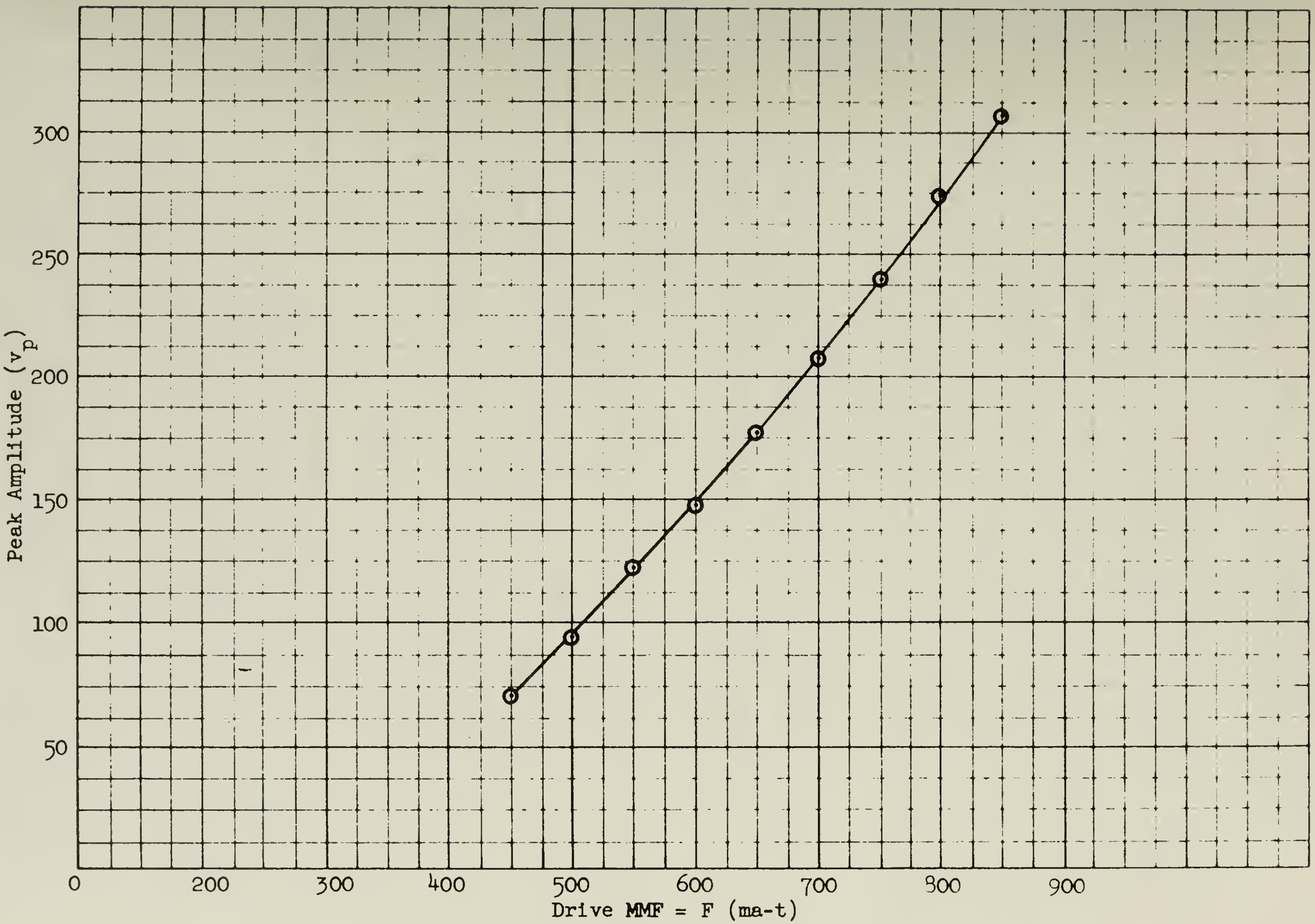

Figure 3.3 Peak Amplitude as a Function of Drive MMF

model. On the other hand, either of the equations is of sufficient accuracy for a number of applications.

A further point should be made concerning the deduction of physical facts from the model(s). The results of the preceding section show that no function of the parameters H, H_o, and S_w (independent of t) could cause the observed non-zero curvature of the inverse switching time curve. It would be tempting, but fallacious, to conclude that since, for example, $H - H_o$ is assumed proportional to the domain wall velocity for the model, then (physical) variations of domain wall velocity cannot be the cause of the observed curvature.

The accuracy of the present model is too poorly established to allow any degree of assurance in predicting physical phenomena.

III.5 Radial Effects

During flux reversal in square-loop cores, the average permeability varies widely with the transient state of magnetization. For a toroid of uniform high-permeability magnetic material, the magnetizing flux is nearly uniformly distributed over any cross-section in the material perpendicular to the flux lines. That is, since $\vec{B} = \mu_o\vec{H} + \vec{M}$ and, in this case, $|\vec{M}| >> |\mu_o\vec{H}|$, the variation of $\vec{H}$ with path length (in agreement with Ampere's law, $F = \oint \vec{H} \cdot \vec{dl}$) is masked by $\vec{M}$.

If the permeability is low, however, $|\vec{M}|$ is of the order of $|\vec{H}|$ so that the flux is more non-uniformly distributed over the core cross-section. Since the field then depends on radius, this state of affairs is called a radial effect.

During switching of a square-loop core, it is clearly quite difficult to determine the inaccuracy involved in assuming a uniform flux distribution.

Although appreciable radial effects do occur experimentally, it is expected that this variation of flux density over core radius can be simulated by an expeditious choice of the statistical distribution of H (or a related quantity such as domain wall velocity).

Two groups of investigators reported, nearly simultaneously, results dealing with radial effects. Tancrell and McMahon (1959) assumed a simple waveform for the switching of a thin annulus of ferrite material, this being of the form of a sinusoid. Integration was performed over radius for various values of parameters, which yields curves closely resembling a full switching curve. Bardezh and Kobelef (1959) report very similar results. Tancrell and McMahon also confirmed their results by drilling small (.005") sensing holes at various radii in a thick-walled core and observing the waveforms of the various layers. The experimental and theoretical switching times were said to agree with calculated values to within 10%.

These results strongly support the case for the existence of radial effects.

If radial effects must be treated, then a statistical approach would seem to offer an attractive alternative to the lengthy integration otherwise required. Using the statistical approach, there would remain some question of the accuracy with which true radial effects could be duplicated.

III.6 Radial Models for Haynes' and Lindsey's Equations

If Haynes' equation is considered as the equation for switching of a differential thickness of core material, the switching waveform for the entire core is:

$$\phi = \frac{\phi_s}{\ell_b - \ell_a} \cdot 6 \left(\frac{1.606}{S_w}\right)^3 t^2 \int_{\ell_a}^{\ell_b} \left(\frac{F}{\ell} - H_o\right)^3 \exp - \left[\frac{1.606}{S_w} t \left(\frac{F}{\ell} - H_o\right)\right]^3 d\ell$$

where ℓ_a, ℓ_b are the inner and outer path length respectively. The above integration yields data typically as summarized in Fig. 3.4. The result of using Haynes' equation for the total core assumed centered at mean radius is shown as a reference. In all cases, H_o and S_w are assumed to be constants.

It can be seen that:

(1) Integration over radius produces no curvature of the inverse switching curve or of the v_p versus F curve (as long as F is large enough to switch the outer radius).

(2) An effect of radial integration is to decrease the peaking time, t_p, and the peak amplitude, v_p, relative to the result of using the same H_o and S_w in Haynes' equation directly.

(3) After integration, the F axis intercepts of the $1/t_p$ and the v_p curves are no longer identical.

These results have proved to be typical for integration over equations of the family defined by (3.4). In particular, this is true for Lindsey's equation.

Result (1) above therefore tends to support the argument that the curvature of the inverse-switching-time curve is not due to radial effects and therefore implies a material effect as the cause. The nature and extent of the various assumptions which have been made in the course of the development do not permit any broad, definite conclusions.

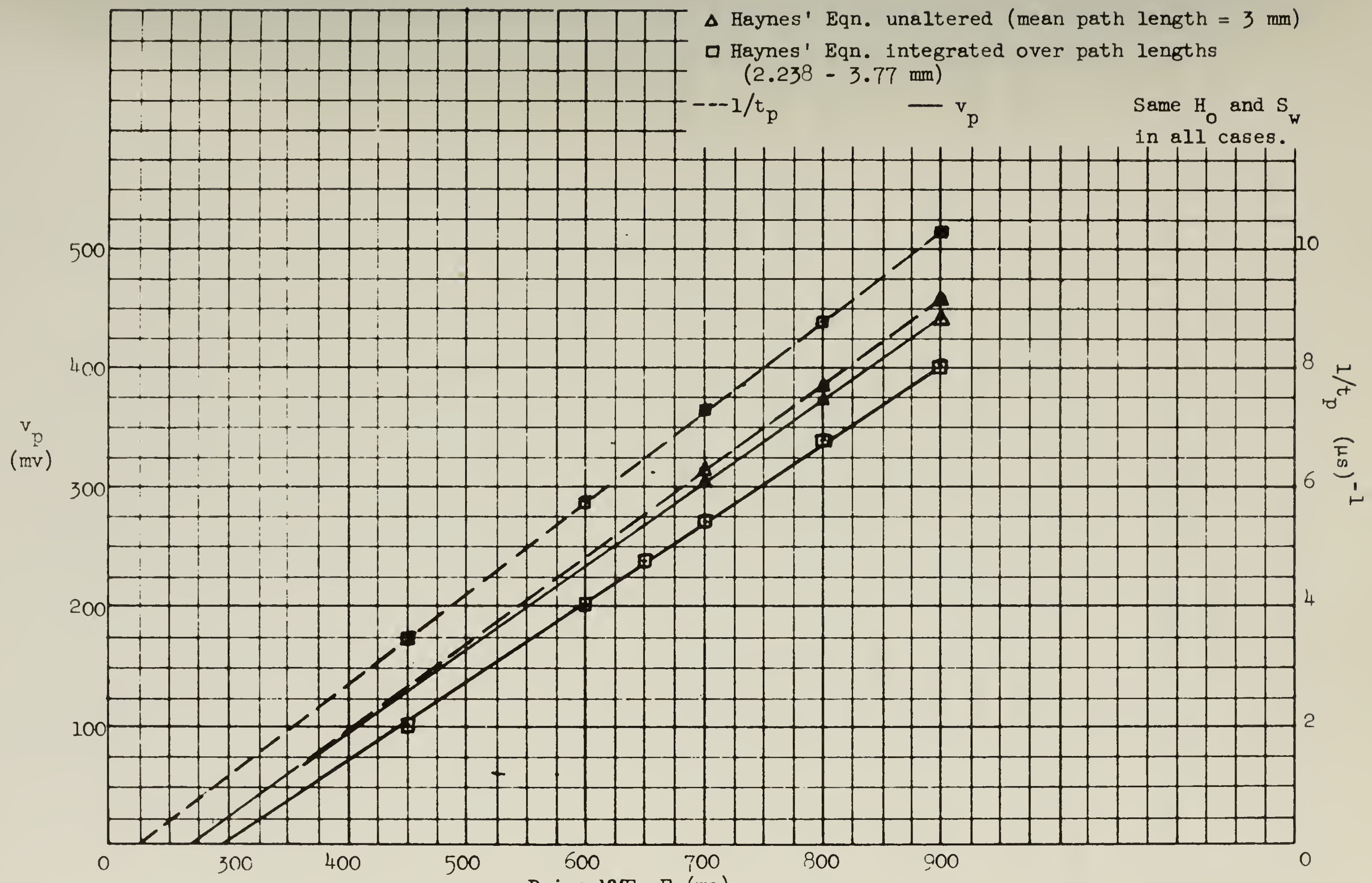

Figure 3.4 Full Switching Radial Effects

Result (2) shows its effect in a larger and longer tail of the switching waveform. That is, since t_p is smaller and v_p is smaller, the constancy of area under the switching curve requires a slower decay of the curve.

The value of $\dot{x}_p t_p$ resulting from integration can be matched within the family of curves defined by (3.4) by choosing a smaller value of n to represent the total core than was used for material alone.

Result (3), however, shows that the integration of a member of (3.4) over radius produces a curve which is not a member of (3.4) since the members of (3.4) have identical F-axis intercepts for the $1/t_p$ and v_p curves. Therefore, it is not possible to exactly account for radial effects by adjustment of n. It is not to be expected that equation (3.4) can yield an arbitrarily accurate switching waveform for a core of any desired radial ratio.

IV. THE MAXPEAK EFFECT

IV.1 Introduction

It was demonstrated in the previous chapter that the full switching models are, to some degree, inexact. The attempt to locate the origin of some of the inaccuracy led to the investigation of partial switching, that is, of flux changes initiated from a non-saturated state.[1] It was expected that the additional information available in partial switching experiments would provide more penetrating information concerning domain activities than would full switching experiments. Thus, the attempt to construct a model of a partial switching effect could be expected to shed some light on the inaccuracies of full switching models.

In order to be useful, the selected partial switching effect should be quite marked and experimentally reproducible. The "maxpeak effect" was found to meet these requirements very well.

The construction of a model of the "maxpeak effect" is the principal objective of the following investigation. In developing this model, we shall endeavor to retain a correspondence between the mathematics and the physical concepts involved, rather than proceed along strictly mathematical lines. It will be shown that a potentially useful model of the maxpeak effect can be developed by logical extension of the concepts of domain activity described by Manyuk and Goodenough (1955) and, in more detail by Haynes (1958) and Lindsey (1959), particularly the latter.

---

[1] The usual meaning of "partial switching" is somewhat broader than the present usage. Usually any flux change substantially less than the maximum possible (twice remanent flux) is called partial switching, regardless of the initial state.

Evidence is presented which supports the idea that a considerable distribution of domain wall velocities (for given driving field) may be involved in the flux reversal process. It is shown that the introduction of such a velocity distribution is harmonious with other relevant data.

Several negative results of the search for a model are also given.

In the following description of experiments, the reproducible saturated state of the core is called the DOWN state. When the core is driven toward the other saturated state, it is said to be switched or driven UP to the UP state.

IV.2 Definition of the Maxpeak Effect

Consider a magnetic core to be driven by a series of pulses as indicated in Fig. 4.1 with the core set to the DOWN state initially.

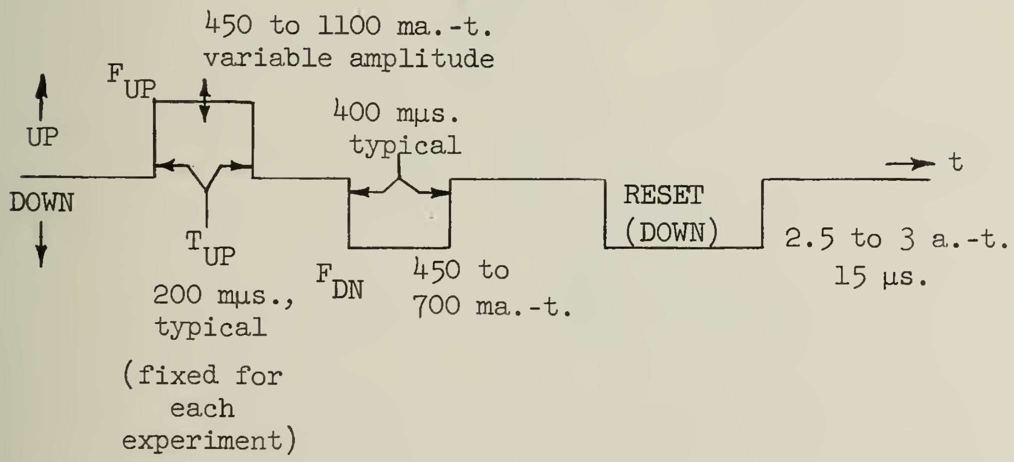

Figure 4.1

As the value of F_{UP} is increased, the core is driven successively closer to the saturated UP state and the sequence of successive switching waveforms due to the DOWN drive is shown in Fig. 4.2 (see also Section IV.4).

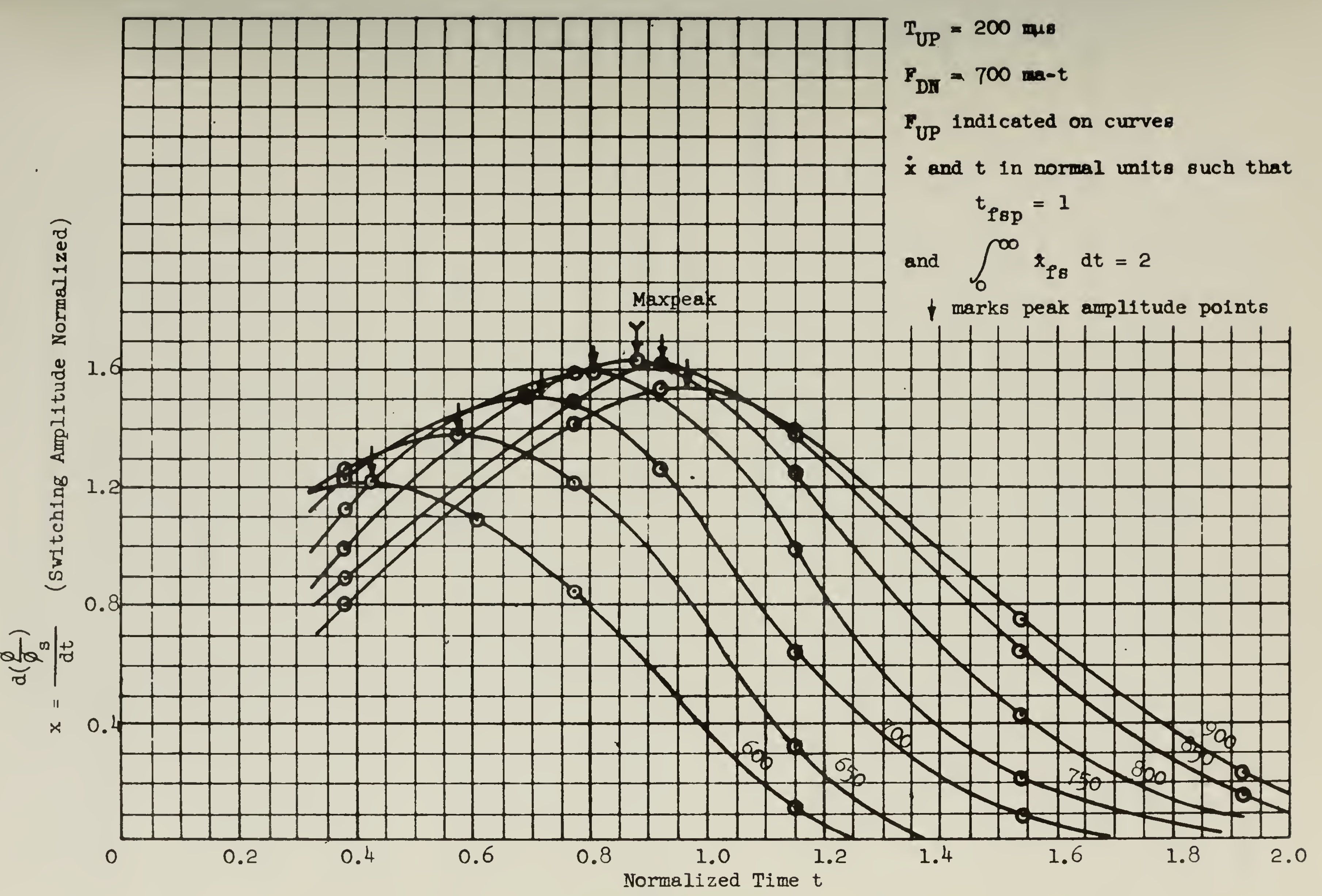

Figure 4.2 Experimental Maxpeak Effect Curves

It can be seen that the peak amplitudes of the curves go through a maximum, in this case, for the amplitude F_{UP} = 800 ma. This peak amplitude is termed the "maxpeak" while the phenomenon is generically named "the maxpeak effect". This effect is, visibly, a substantial one, the maxpeak amplitude being some 30 - 90% greater than the full-switching peak amplitude (for the same F_{DN}).

For the present, we shall only consider the maxpeak effect at higher values of F_{DN} (corresponding approximately to $2H_o \approx 700$ ma. -t).

In all subsequent work, rectangular current pulses having rise times of 1 mμsec. (hence only 0.5% of the average switching time) are used. The RESET drive, for which only peak amplitude and duration are critical, has a somewhat slower risetime (see Appendix I).

IV.3 Previous Investigations

Smith (1960) is the only investigator known to have published any data concerning the maxpeak effect. His experiments were performed on a specially prepared thin - wall core having an OD/ID ratio of 1.2. The material of the core is probably very similar to that of the core used in the present study, a MgMn ferrite (see Appendix I). The conclusions which Smith reaches concerning this effect are:

(1) the difference, (maxpeak amplitude)-(full switching peak amplitude) = a constant, viz., 60 mv. over a wide range of drives.

(2) the maxpeak curve contains 90% of the total flux of the core i.e., maxpeak occurs for the condition that 90% of the total flux was switched during the UP pulse in all cases.

His investigation, not being concerned with models, proceeds only to the point of stating the above observations and some general comments on the possible origin of this effect.

IV.4 Experimental Results

Fig. 4.3 presents curves of the peak amplitudes of switching curves under various conditions of F_{UP} and T_{UP} for a given F_{DN}. It is immediately seen that the difference $v_{maxpeak} - v_{full\ switching\ peak}$ is remarkably close to the value given by Smith. In the present case, the values are 69, 74, and 58 mv. (average 67 mv.) respectively as compared to Smith's value of 60 mv., in spite of the difference in OD/ID ratio of the cores used in the two investigations (Smith 1.2; present, 1.68).

We now introduce the symbolism defined by Fig. 4.4.

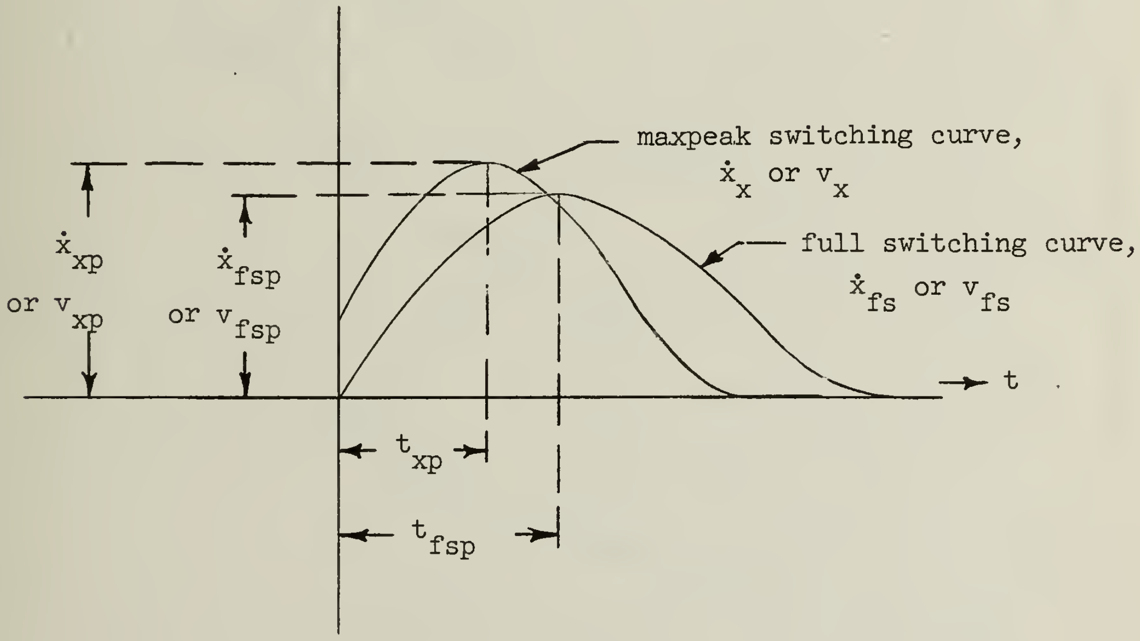

Figure 4.4

From the experimental data, we deduce the following statements concerning the maxpeak switching curve.

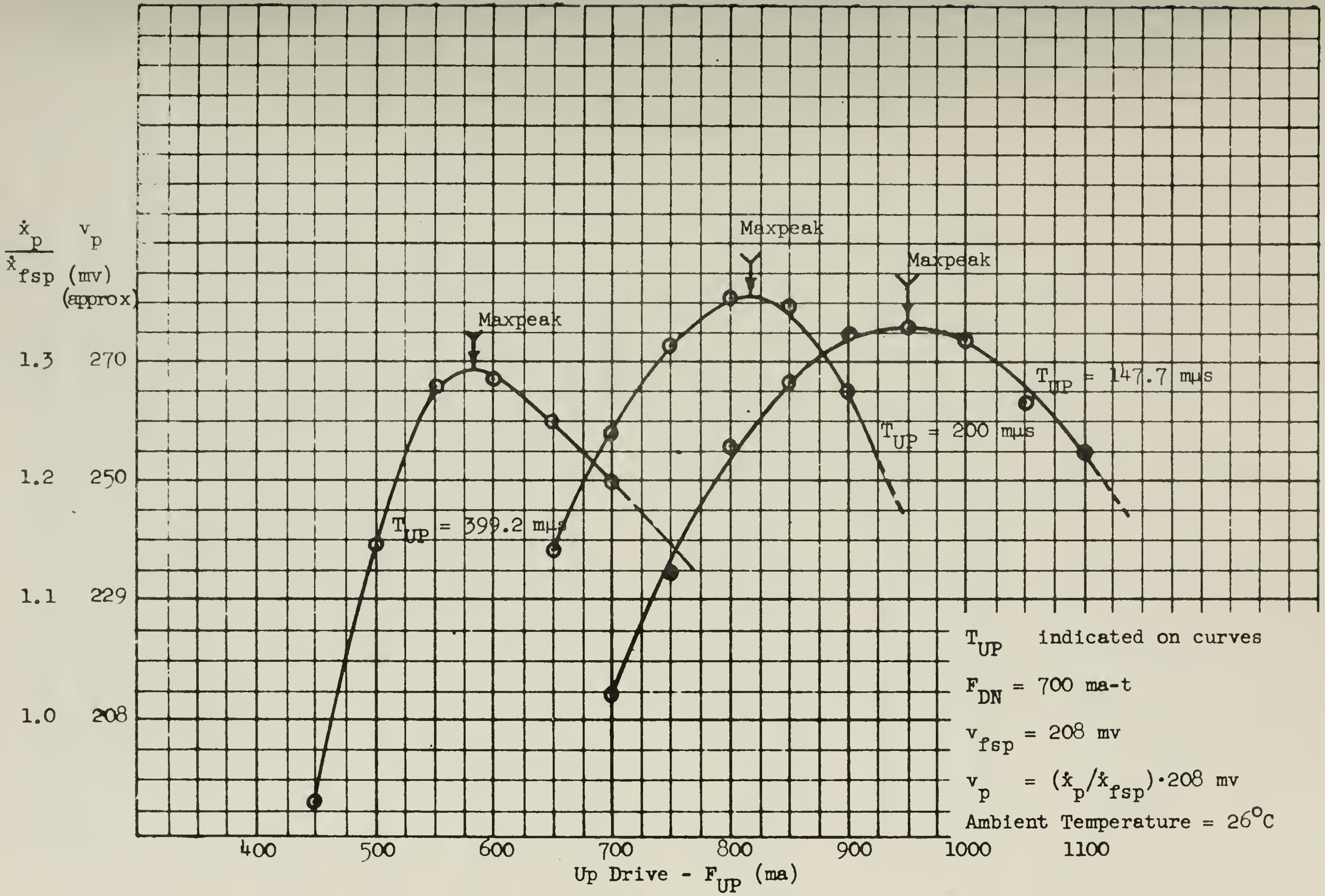

Figure 4.3 Envelope of Peak Amplitudes of Maxpeak Effect Curves

$$(1) \qquad \int_0^\infty \dot{x}_x \, dt \cong 0.83 \int_0^\infty \dot{x}_{fs} \, dt$$

$$(2) \qquad \frac{\dot{x}_{xp}}{\dot{x}_{fsp}} \cong 1.3 \qquad \text{near } F_{DN} = 2H_o \cong 700 \text{ ma.}$$

$$\text{in present case.}$$

$$(3) \qquad t_{xp} \cong 0.88\, t_{fsp} \qquad (4.1)$$

It should be noted that for (1) above, Smith would have 0.9 rather than 0.83. Since Smith concludes that $\dot{x}_{xp} - \dot{x}_{fsp}$ = constant, there is no exact equivalent to (2) above. Also, no relation of the variables of (3) above is given by him.

In a later section, evidence will be presented which demonstrates that neither relation (2) or (3) holds over extensive ranges of F_{DN} and that Smith's relation $\dot{x}_{xp} - \dot{x}_{fsp}$ = constant is likewise inadequate.

IV.5 The Formulation of a Model

The object of the following investigation is to discover a model of switching which describes the maxpeak effect. The principal constraint in this inquiry is that the model be based on switching processes which are either known or are reasonable on the basis of present evidence. Stated negatively, purely mathematical models, having no known relation to physical factors, are specifically disallowed.

It is, of course, desirable that any such model be as simple as possible within certain accuracy limitations. A case in point is the lingering question of radial effects. If they must be introduced exactly the mathematical complexity is greater due to the lengthy integration which ensues. It is desirable, on the other hand, to account for radial effects statistically. Both the exact and statistical approaches are subject to consideration, however.

IV.6 The Maxpeak Effect on the Basis of Radial Effects Only

Prior to the publication of Smith's work, the possibility that the maxpeak effect is due solely to radial effects was considered. For this investigation, switching curves of the family of equations (3.3) and (3.4) were used. It is assumed that the switching curve followed by a given annulus of the core is the final portion of the full-switching curve which would have been followed if switching had commenced at saturation. The following equations apply.

During UP drive

$$\dot{x}_u = 2nK_u^n t_u^{n-1} e^{-(K_u t_u)^n}$$

$$x_u = 1 - 2e^{-(K_u t_u)^n} \qquad 0 \leq t_u \leq T_u$$

At termination of UP drive

$$\dot{X}_u = 2n\,K_u^n T_u^{n-1} e^{-(K_u T_u)^n}$$

$$X_u = 1 - 2e^{-(K_u T_u)^n} \qquad t_u = T_u$$

During DOWN Drive

$$\dot{x}_d = -2n\,K_d^n\,(t_d + \tau)^{n-1}\, e^{-[K_d(t_d + \tau)]^n}$$

$$x_d = -1 + 2e^{-[K_d(t_d + \tau)]^n}$$

$$\text{where } \tau = \frac{1}{K_d}\left(-\ln \frac{1 + X_u}{2}\right)^{1/n} \qquad t_d \geq 0$$

Subscript u corresponds to UP, d to DOWN. Capitals $(X, \dot{X}, T)$ imply final values.

These equations are then integrated (see Appendix II) over values of K_u and K_d corresponding to the various rings into which the core is divided. By adjusting H_o, S_w, and n, it is possible to obtain results similar to those of Fig. 4.3.

Fig. 4.5 is a case in which the curve for n = 3 provides a remarkably good fit to the experimental data. In all cases, the values of H_o and S_w are adjusted such that

(1) the absolute maxpeak amplitude is correct and

(2) the maxpeak occurs at the correct value of F_{DN}, the driving m.m.f. in the DOWN direction.

The t_p curves for n = 3 and n = 4 are quite tolerably near the experimental curve while for n = 2, the agreement is poor. Also for n = 3, the absolute full-switching peak amplitude is in good agreement. However, when this model is applied to the case of maxpeaking arising from other values of T_{UP}, it is found that the required value of H_o becomes physically unreasonable. This fact alone leads to the conclusion that the maxpeak effect is probably not physically ascribable to radial effects only.

Further confirmation of this conclusion is given in Section IV.9.

IV.7 Basic Model of Maxpeak Effect

From the similarity of Smith's results with the present results, as indicated in Section IV.4, it is logical to assume that the maxpeak effect depends principally upon microscopic magnetic properties rather than macroscopic ones. An extension of Lindsey's model to explain this effect will now be considered. (Lindsey's model is used because the results of Section III.3 indicate n = 2 agrees best with full-switching data.)

The equation of the full-switching curve for n = 2 may be written:

$$\dot{x} = 4K^2 t \; e^{-K^2 t^2} \qquad (4.3)$$

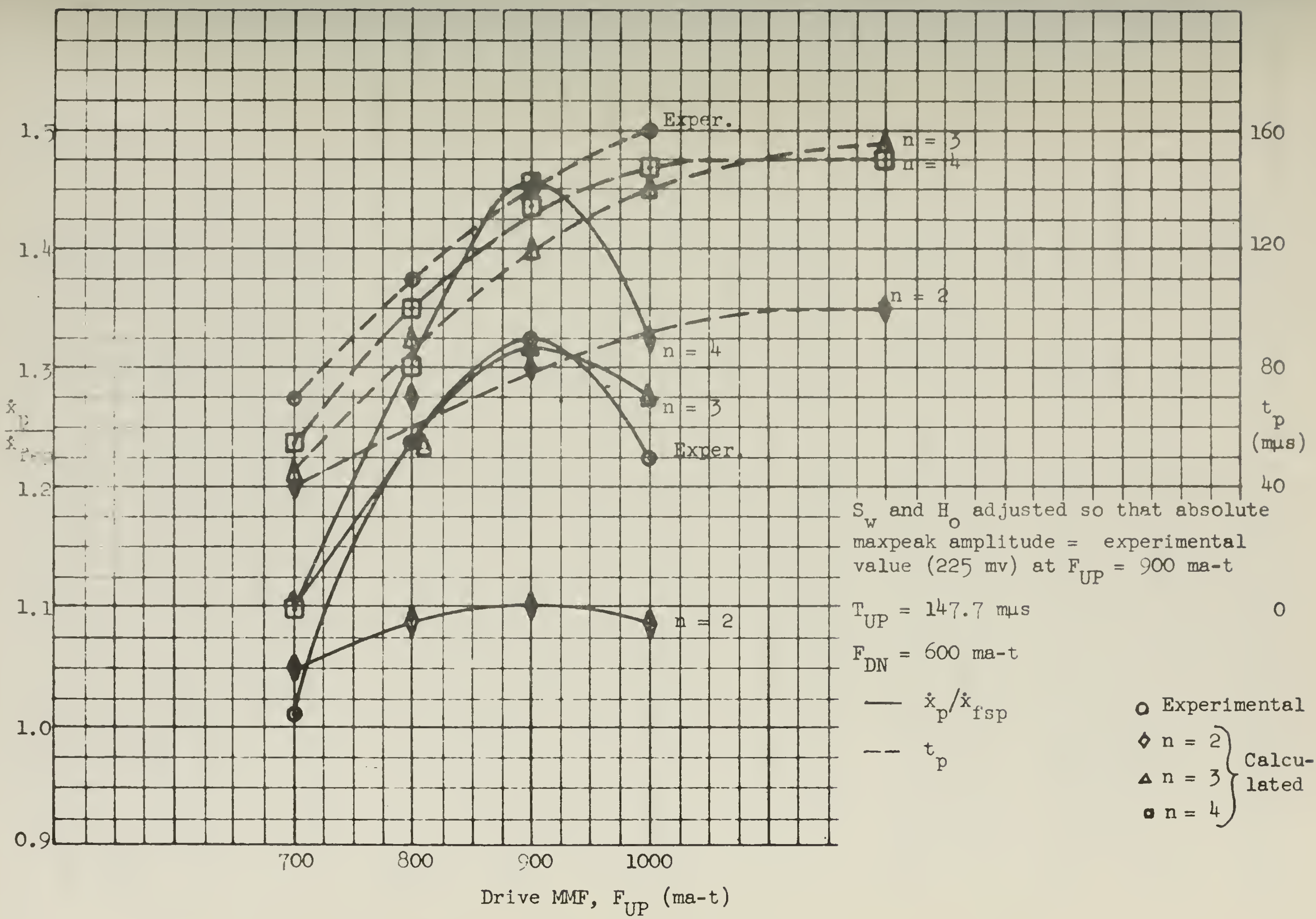

Figure 4.5 Envelope of Maxpeak Effect Curves
(Calculated Curves include Integrated Radial Effects Only)

Examination of the derivation of this equation shows the following significance of the various terms:

K is the domain wall velocity in sec.$^{-1}$; that is, the velocity normalized to length units of core size; or, if preferred, $1/K$ is time required for the fraction, $1-e^{-1}$, of the flux to be reversed.

$4K^2t$ is the time rate of transfer of cross-sectional core area ($\sim$ flux) to the new direction if no domain wall collisions occur.

$e^{-K^2t^2}$ is the probability of a domain wall having not yet been annihilated at time t; or, the fraction of nucleating centers whose walls are still "active" at time t.

Consider a cross-section of polycrystalline material having been switched such that the domain walls are as indicated in Fig. 4.6a. Some domains have stopped growing (according to either Lindsey's or Haynes' model) at small radius, others at larger radius (type α) and still others (type β) would continue to grow if the field were not removed at time T_{UP}. Upon application of a sufficiently large drive field in the direction H_{DN}, it is assumed that

(a) inactive domains (type α domains) simply renucleate from their original nucleating centers.

(b) active domains (type β domains) both renucleate from their original centers and the existing domain wall is also pushed inward, preserving its circular geometry. Domains in this class, when subjected to the DOWN pulse will deliver flux in a way shown by the following analysis.

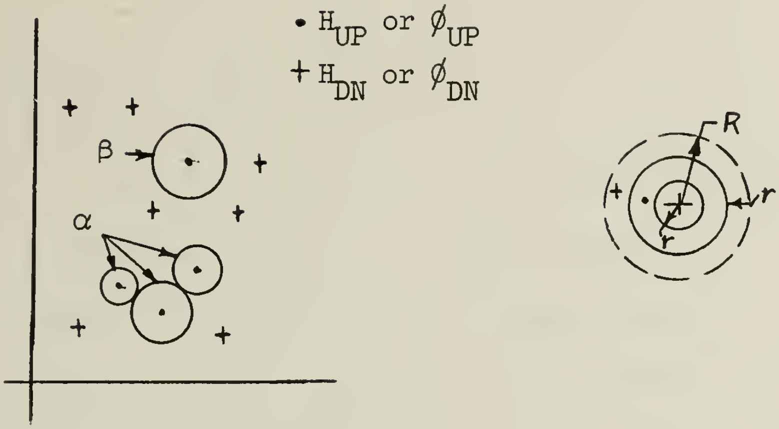

(a) (b)

Figure 4.6

Referring to Fig. 4.6, if R is the radius of the domain at time T_{UP}, then at some time during the DOWN pulse, the radius of the outer wall will be (R-r) while the newly renucleated inner wall is at radius r since the velocity of inner and outer walls is equal. The total length, ℓ, of domain wall at this time is:

$$\ell = 2\pi r + 2\pi(R-r) = 2\pi R$$

Since $\frac{dA}{dt} = v\ell$, where v is the wall velocity, it can be seen that $\frac{dA}{dt}$ and, therefore, $\frac{d\phi}{dt}$ is constant, for this type of domain activity until the inner and outer walls collide. This latter condition corresponds to $r' = \frac{R}{2}$ which, since $R = K_u T_u$ while $r' = K_d t'_d$, can be written,

$$K_d t'_d = \frac{K_u T_u}{2} \tag{4.4}$$

t'_d being the time of annihilation of the two counter-moving β-domain walls.

Meanwhile, the walls renucleated from α-type centers in Fig. 4.6a simply retrace the flux reversal procedure of the previous UP pulse.

IV.8 Analysis of the Basic Model

The model proposed for the maxpeak effect can now be conveniently examined graphically. (The exact description is given by equations (4.5)). The details of this graphical method will be demonstrated by the use of Fig. 4.7. Since the quantity K_u/K_d[2] is only a scaling factor of the amplitude and time, setting $K_u/K_d = 1$ greatly simplifies the presentation.

In Fig. 4.7, the two components of flux which have been reversed at time T_u are indicated as the shaded areas in the upper diagram. The flux transfer during the DOWN drive is, of course, the chief concern. The amplitude, $\dot{x}_d$, is actually of opposite sign to $\dot{x}_u$ but is shown the same for convenience. During the DOWN drive, the flux change is hypothesized to consist of two parts, the α and the β domain contributions. The former contribution has precisely the same waveform during the UP and the DOWN drive (remembering the assumption $K_u = K_d$).

The contribution of the β domains is, itself, composed of two parts. The inner walls (renucleated walls) contribute a component of flux exactly equal to the contribution of β domains from time $t = 0$ to $t = T_u/2$ (see below) during UP drive. The outer β domain walls (those already nucleated and not annihilated during the UP drive) contribute the reaminder of flux delivered by β domains. The total time rate of flux change during DOWN drive is the sum of the α and β contributions as indicated in Fig. 4.7.

At time $T_u/2 = t_d'$, the inner and outer β domain walls collide since, as shown in the previous section, $t_d' = K_u T_u/2K_d$ which is just $T_u/2$ when $K_u = K_d$.

---

[2] Subscript "u" refers to UP drive, "d" to DOWN drive.

$K_{UP} = K_{DN}$ or $F_{UP} = F_{DN}$; $n = 2$

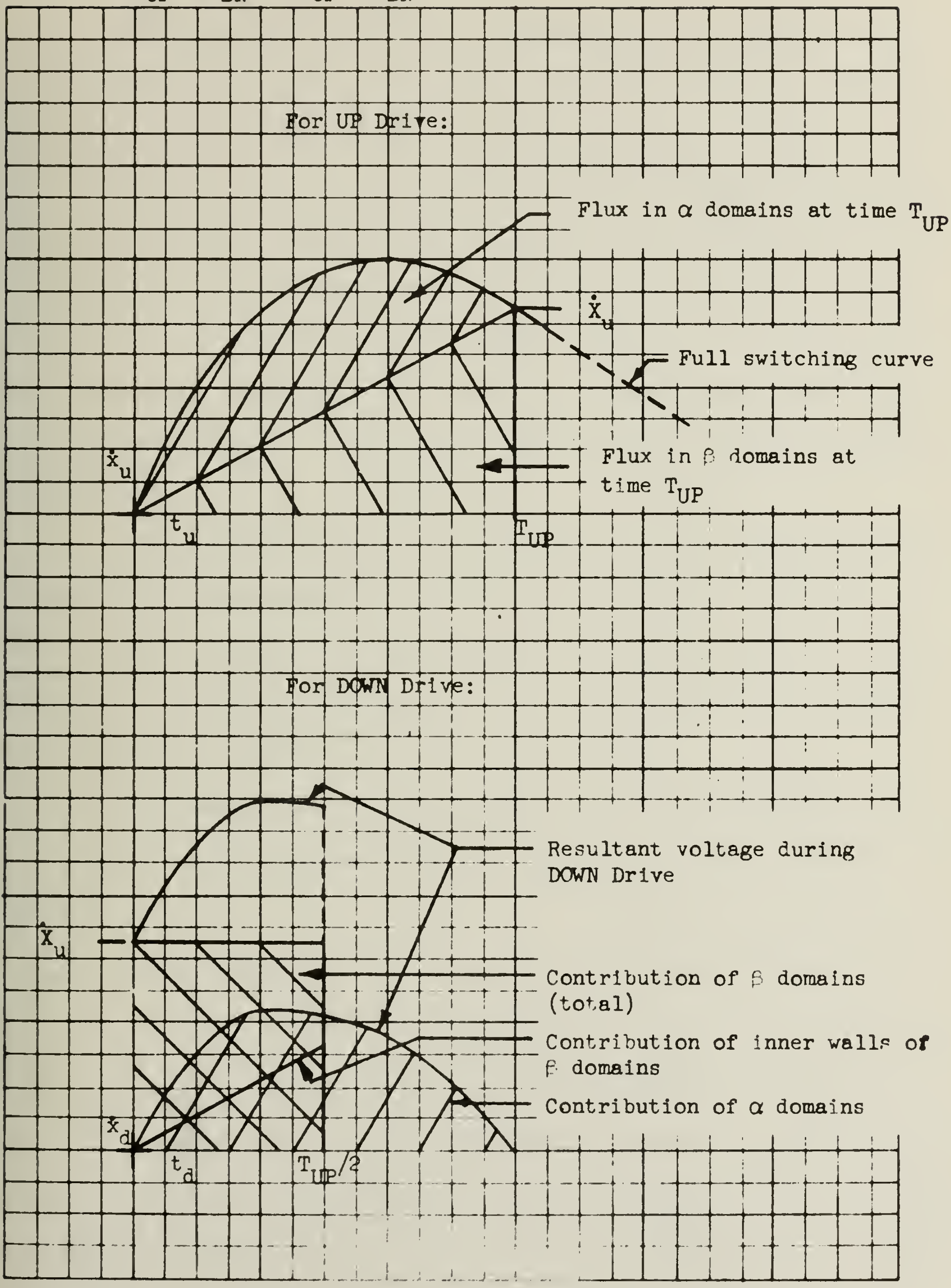
For UP Drive:
Flux in α domains at time T_{UP}
$\dot{x}_u$
Full switching curve
$\dot{x}_u$
Flux in β domains at time T_{UP}
t_u
T_{UP}
For DOWN Drive:
Resultant voltage during DOWN Drive
$\dot{x}_u$
Contribution of β domains (total)
Contribution of inner walls of β domains
Contribution of α domains
$\dot{x}_d$
t_d
$T_{UP}/2$

Figure 4.7 Graphical Construction of Maxpeak Effect Curves for Basic Model

The preceding description corresponds to some single set of F_u (or K_u), F_d (or K_d), and T_u. In order to obtain the family of curves for the maxpeak effect similar to Fig. 4.2, the value of F_u (or K_u) is usually varied while T_u and F_d are held constant. For the purposes of graphical analysis, it is much simpler to vary T_u than F_u. It is possible to interchange these two variables because, for a given n, Kt always occurs as a product in the switching equation (Eq. 3.4) except for a multiplier of K. This multiplier, therefore, simply scales the absolute magnitudes of the amplitude and time axes. It has been tacitly assumed that n is the same for F_u and F_d.

The maxpeak effect curves corresponding to the "basic" model of the maxpeak effect, constructed by the method indicated, are presented in Fig. 4.8. The resultant curves, numbered 1 to 3, are each constructed as explained in connection with Fig. 4.7. It can be seen that the maxpeak curve is number 2 whose peak amplitude is 1.33 $\dot{x}_{fsp}$.

Several differences between the maxpeak curve deduced from the model and that found experimentally are apparent. The model predicts maxpeak:

(1) at a value of flux which is too small ($\approx$ 63% rather than 83% of the total flux),

(2) at a time which is too early relative to t_{fsp}.

Also, the wall collapse of β domains shows a deterministic fall of voltage which is not observed experimentally. In this connection, it is also noted that Smith's curves (for a thin core) show voltage falls no more precipitous than for a thick core, suggesting that smoothing due to radial effects is not the principal factor in removing the sharp drop predicted by the basic model.

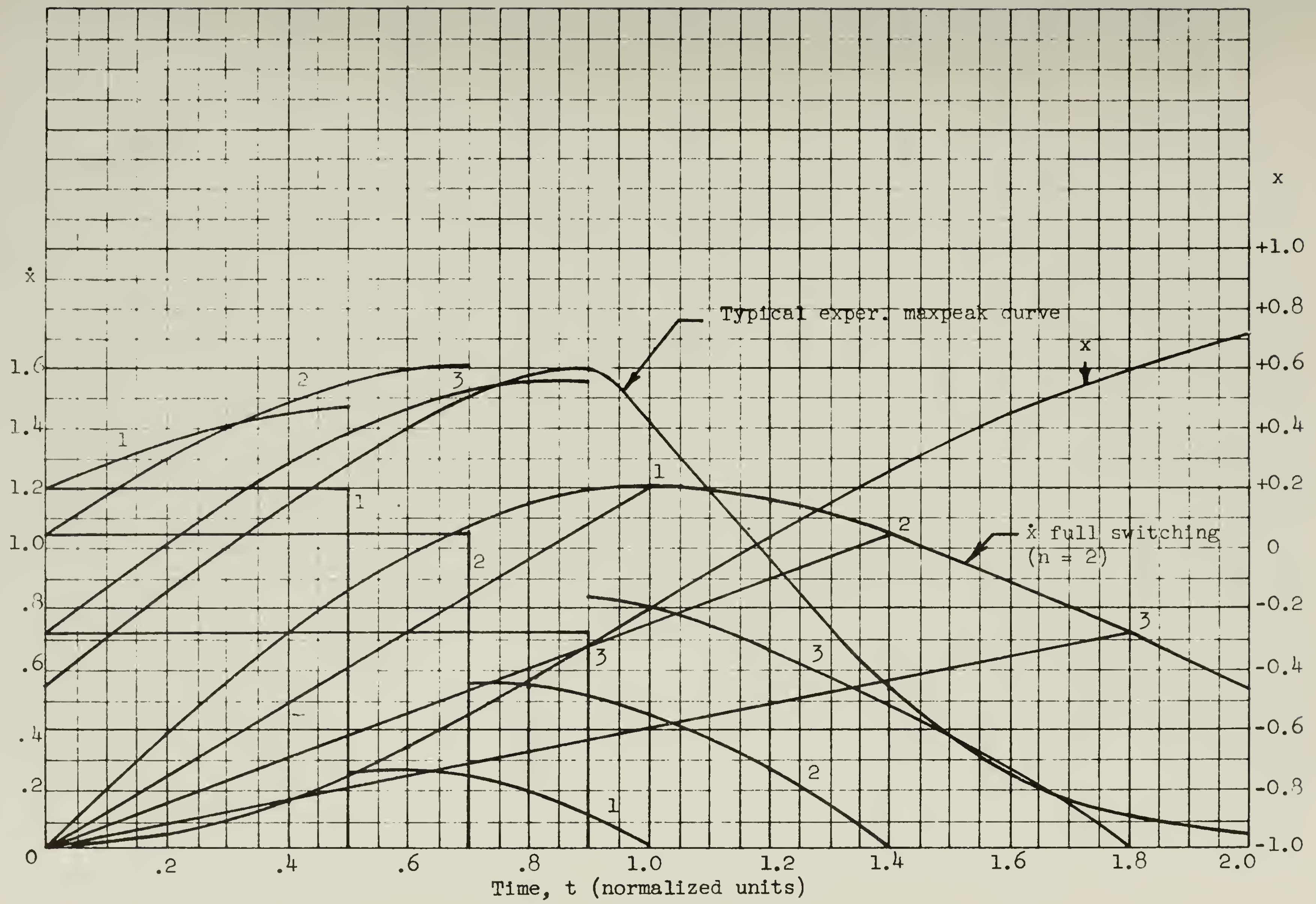

Figure 4.8 Maxpeak Effect Curves - Basic Model

On further examination it is found that only $\approx 4\%$ of the total flux would have to be shifted under the curve given by the model in order to match the experimental maxpeak curve (using the model-derived curve which includes the same total area as the experimental curve).

In summary, the basic maxpeak effect model, which is a logical extension of Lindsey's model, has several shortcomings when compared against the absolute standard of experimental data. Positive results are also present, the most outstanding being the maxpeak amplitude ratio $\dot{x}_{xp}/\dot{x}_{fsp} = 1.33$ according to the model as compared to 1.30 to 1.36 for various experimental cases (Fig. 4.3) for relatively large F_{DN}.

The equations for the basic maxpeak model are as follows:

$$\dot{x}_d = 4K_d^2 t_d \, e^{-K_d^2 t_d^2} - \left(\frac{K_d}{K_u}\right)^2 \frac{\dot{X}_u}{T_u} t_d + \frac{K_d}{K_u} \dot{X}_u \qquad \text{for } 0 \leq t_d < \frac{K_u T_u}{2 K_d}$$

$$\dot{x}_d = 4K_d^2 t_d \, e^{-K_d^2 t_d^2} - \left(\frac{K_d}{K_u}\right)^2 \frac{\dot{X}_u}{T_u} t_d \qquad \text{for } \frac{K_u T_u}{2 K_d} < t_d \leq \frac{K_u T_u}{K_d}$$

or, more briefly,

$$\dot{x}_d = \dot{x}_{d_{fs}} - \frac{\dot{x}_d(0)}{2\, T_d'} t_d + \dot{x}_d(0) \qquad \text{for } 0 < t_d < T_d'$$

$$\dot{x}_d = \dot{x}_{d_{fs}} - \frac{\dot{x}_d(0)}{2\, T_d'} t_d \qquad \text{for } T_d' < t_d \leq 2T_d'$$

where

$$\dot{x}_{d_{fs}} = 4K_d^2 t_d \; e^{-K_d^2 t_d^2}$$

$$\dot{x}_d(0) = \dot{x}_d\,(t_d = 0) = \left(\frac{K_d}{K_u}\right) \dot{X}_u = \left(\frac{K_d}{K_u}\right) [4K_u^2 T_u \; e^{-K_u^2 T_u^2}]$$

$$T_d' = \frac{K_u T_u}{2\,K_d}$$

and

$$K = 1.606 \left(\frac{H - H_o}{S_w}\right)$$

IV.9 Modification of the Basic Model by Wall Velocity Distribution

In order to obtain a more accurate model for the maxpeak effect, various modifications of the basic model will be considered.

The deterministic fall of voltage which the basic model predicts is of immediate concern. Studies (e.g., LFE 1960)) of thin metallic films have shown that variations in the velocities of domain walls occur both for individual walls as functions of position and for all walls collectively. Such variations may be due to composition gradients of various kinds. There is insufficient data available, however, to adequately assess the magnitude of this effect.

Calculations have been made (similar to Section IV.8) in order to examine the effect of velocity variation on the maxpeak effect curves. It is supposed that the time of collapse of the β domains is normally distributed about time $\frac{K_u T_u}{2\,K_d}$ and with standard deviation $\sigma = 0.2\,(\frac{K_u T_u}{2\,K_d})$. The resulting set of curves is given in Fig. 4.9.

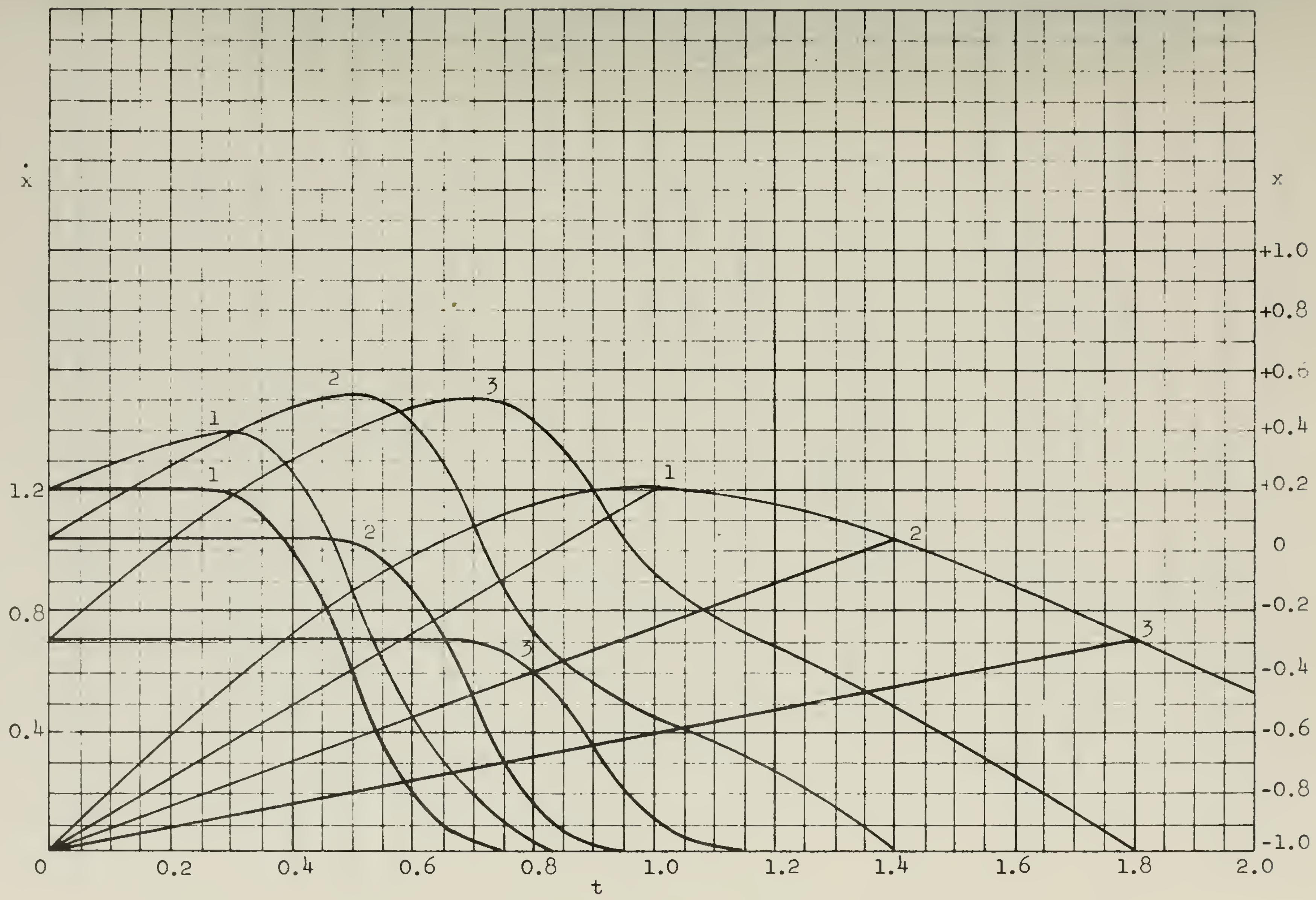

Figure 4.9 Maxpeak Effect Curves with Velocity Distribution $\sigma = 0.2K_{mean}$, n = 2

The corresponding velocity distribution should, for consistency, also be introduced into the full-switching equation. The resulting full-switching curve is shown in Fig. 4.10. It is evident that the error thereby introduced is negligible.

A measure of the relative accuracy of the maxpeak model is afforded by the average absolute value of the error as a percentage of peak amplitude.[3] Thus,

$$A = \frac{1}{n} \sum_{i=1}^{n} \frac{\left| v_T(t_i) - v_{EX}(t_i) \right|}{v_{EX}(t_p)} \cdot 100\%$$

where $v_T(t_i)$ is the theoretical voltage at time t_i and $v_{EX}(t_i)$ is the experimental voltage at time t_i.

For the data of Fig. 4.9, $A \cong 6.5\%$ is found for a typical maxpeak curve. By comparison, a full-switching curve from the family of equation (3.4) compared to a fitted experimental full-switching curve corresponds to $A \cong 2\%$.

Therefore, the maxpeak effect model with velocity smoothing is reasonably accurate. It should be pointed out, however, that other highly sensitive measures of accuracy of the model show that some problems remain. Namely, the model predicts the maxpeak at a flux level which is too small (approximately 70% rather than 83%). Also, t_{xp}/t_{fsp} is too small (0.55 as compared to 0.88).

---

[3] This measure tends to emphasize voltage errors in accordance with the interests of engineering applications.

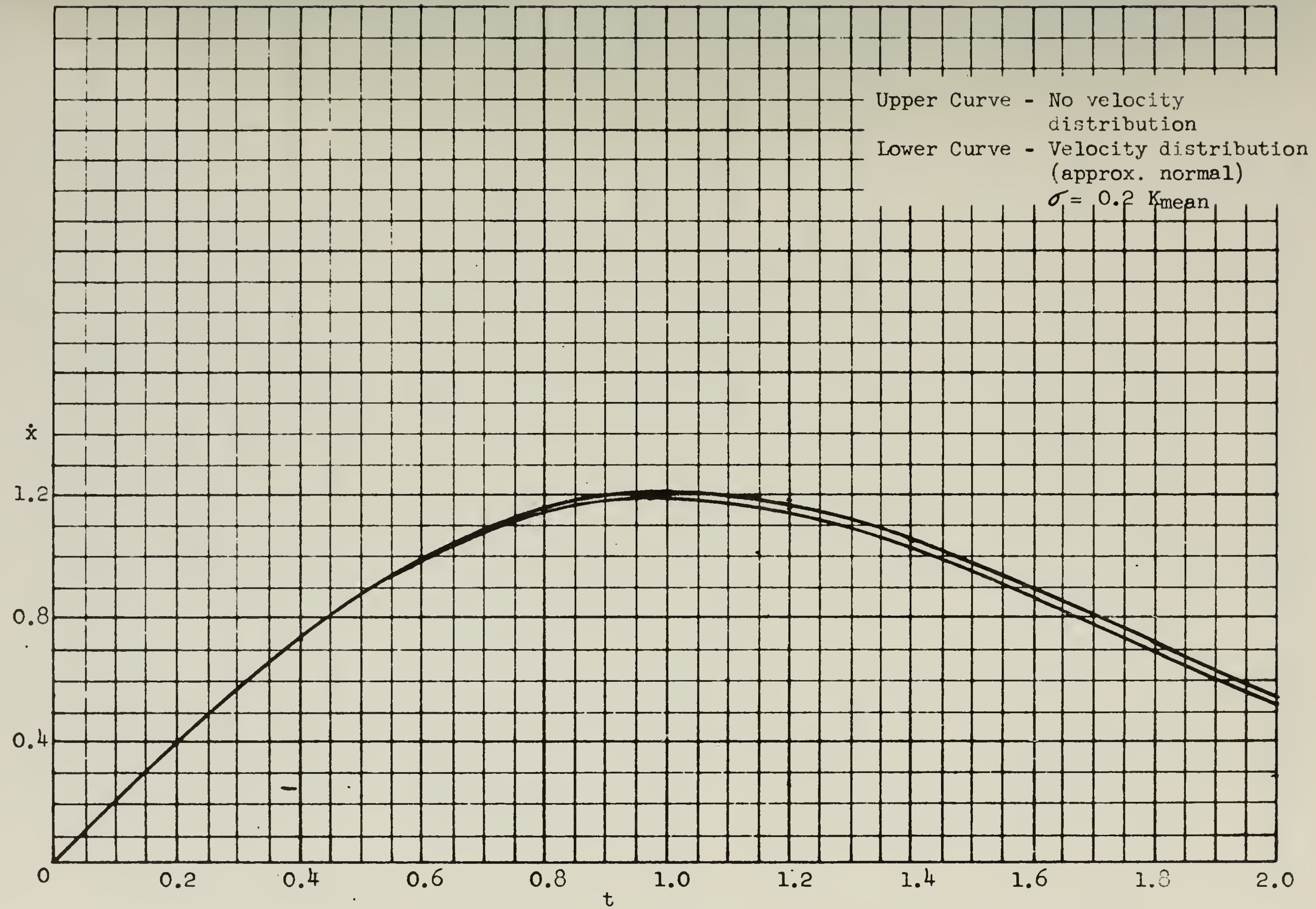

Figure 4.10 Full Switching Curves for $n = 2$ with and without Normal Velocity Distribution

The equation for the maxpeak model with velocity distribution is as follows:

$$\dot{x}_d = 4K_d^2 t_d \, e^{-(K_d t_d)^2} - \left(\frac{K_d}{K_u}\right) \cdot \frac{\dot{X}_u}{T_u} t_d + \frac{K_d}{K_u} \dot{X}_u \left\{ 1 - \int_{-\infty}^{t_d} \frac{1}{\sqrt{2\pi}\,\sigma} \, e^{-\frac{(y - T_d')^2}{2\sigma^2}} dy \right\}$$

$$\text{for } t_d \geq 0$$

All quantities are as defined in Section IV.8 with the addition that $\sigma = 0.2\, T_d'$ is adequate.

IV.10 Modification of Basic Model by Radial Effects

In previous sections of this chapter, it has been demonstrated that radial effects are unlikely to be either the principal source of the maxpeak effect of the cause of smoothing of the basic maxpeak model. The main support is derived from the fact that the maxpeak curve shown by Smith for a core of radial ratio 1.2 is not notably different from present curves for a radial ratio of 1.68; hence, the radial ratio is probably not a principal factor.

This viewpoint is corroborated by the following argument. Let us assume that the basic maxpeak model holds for an annulus of core material and that $H = \frac{F}{\ell}$ is the field intensity due to the mmf F applied to core path length ℓ, i.e., to the annulus at radius $\ell/2\pi$.

Consider the condition when $F_{UP} = F_{DN}$. Then the time at which β domains collapse is $t_d' = \frac{K_u T_u}{2 K_d}$ for each annulus individually. Since

$K_u = \frac{1.60\dot{6}}{S_w}(\frac{F_{UP}}{\ell_i} - H_o)$ and $K_d = \frac{1.60\dot{6}}{S_w}(\frac{F_{DN}}{\ell_i} - H_o)$ for annulus i, then for any i, $t'_d = \frac{T_u}{2}$ = a constant for all i. (H_o and S_w are always assumed independent of radius.) Therefore, when $F_{UP} = F_{DN}$, the collapse of β domains should occur simultaneously in all annulae which does not, in fact, occur as reference to Fig. 4.2 will demonstrate. Thus, radial smoothing alone cannot remove the deterministic fall of potential which occurs in the basic model.

The point is that for one case ($F_u = F_d$) in each family of maxpeak effect curves, the time of collapse of β domains must be the same in all annulae. In that case, a sharp fall of potential is predicted if the "basic" maxpeak effect model is used for each annulus. Thus, in one (usual) case, radial smoothing is completely ineffective.

By extension of the foregoing argument, it is seen that the predicted maxpeak effect curves for the total core must, under the described conditions, be the same as that of any single annulus. Therefore, the maxpeak model assumed to hold for an ideal thin core, whatever it may be, will apply to a core independent of its radial dimensions.

V. THE MAXPEAK EFFECT FOR WIDER RANGE OF F_{DN}

V.1 Experimental Results

In the previous sections, we have examined the maxpeak effect for particular large values of F_{DN}. The only relation which has been found to hold independent of F_{UP}, T_{UP} and F_{DN} is the percentage of flux corresponding to maxpeak, namely,

$$\int_0^\infty \dot{x}_x \, dt = 0.83 \int_0^\infty \dot{x}_{fs} \, dt \qquad (5.1)$$

For a wide range of F_{DN}, it is found that $v_{xp} - v_{fsp}$, $\dot{x}_{xp}/\dot{x}_{fsp}$, and t_{xp}/t_{fsp} vary with F_{DN} as shown in Fig. 5.1. For these experiments, F_{UP} and T_{UP} are held constant in order to satisfy the conditions of equation (5.1).

(a) $v_{xp} - v_{fsp}$ is an increasing function of F_{DN}.

(b) $\dot{x}_{xp}/\dot{x}_{fsp}$ is a decreasing function of F_{DN}.

(c) t_{xp}/t_{fsp} is an increasing function of F_{DN}.

Statement (a) is in disagreement with the results of Smith who, as previously noted, finds $v_{xp} - v_{fsp}$ = constant. The difference between Smith's findings and the present ones may be due to any of a large number of causes such as inaccuracies in measurement in either or both investigations, radial effects, or true differences in the magnetic materials employed.

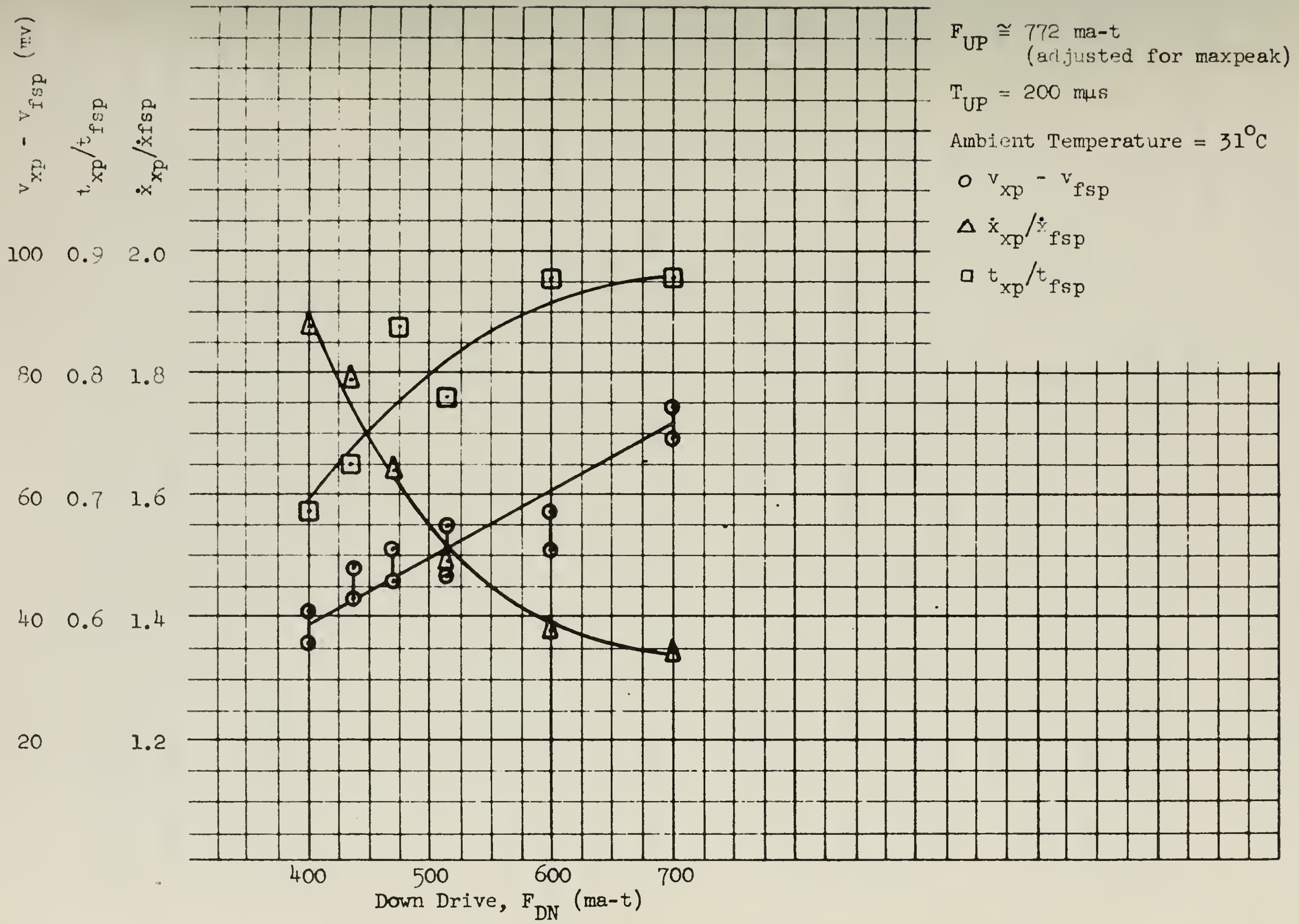

Figure 5.1 Various Maxpeak Quantities as a Function of F_{DN}

Statement (b) agrees with Smith and his unreduced data appears to support statement (c).

V.2 Maxpeak Effect at Low F_{DN}

It would now be desirable to construct a switching model which holds over a wider range of F_{DN} than the basic model. For this objective, it is reasonable to attempt to broaden, in some sense, the basic model. Let us point out that this goal has been only partially successful.

Also, much of the following discussion should be considered more speculative than the preceding work. In particular, the members of the class of domain shapes and wall motions which could lead to certain macroscopic results are clearly vast in number. Hence, notions corresponding to this class should be regarded, primarily, as symbolic or hypothetical.

The argument which will be examined is, briefly, that the large values of $\dot{x}_{xp}/\dot{x}_{fsp}$ for small F_{DN} are strongly related to the curvature of the $1/\tau_s$ versus F (or v_p vs. F) curve of Fig. 3.3. It was shown in Chapter III that curvature of the v_p vs. F curve for full switching corresponds to increasing values of $\dot{x}_p t_p$ with F. Within the confines of the family of curves defined by

$$x_n = 1 - 2 \exp [-(Kt)^n] \tag{5.2}$$

of which Haynes' and Lindsey's equations are members, variations in $\dot{x}_p t_p$ were shown to depend only on n. In the range of F which is now being considered (ca. 400-700 ma.), the corresponding values of n were found to be about 1.8 to 2.2. The meaning to be ascribed to non-integer n is now considered.

The case n = 2 corresponds to cylindrical domain growth, according to Lindsey's model, which, neglecting wall annihilations, may be equivalently stated $L \propto t^1$ where L is the total domain wall length t being, as usual, time and step function drive being assumed. Similarly, n = 3 corresponds to ellipsoidal domain growth for which $L \propto t^2$. Therefore n = 1 will be assumed to correspond to constant wall length, i.e., $L \propto t^0 = 1$.

For $1 < n < 2$, it will be assumed that a general domain increases its wall length in accordance with n = 2 (that is, $L \propto t^1$) for some portion of its life and in accordance with n = 1 (that is, $L \propto t^0$) for the remaining portion of its life. The resulting rate of flux reversal in the absence of wall collisions is proportional to t^{n-1} where $1 < n < 2$. For $2 < n < 3$, the reversal process may be assumed as a combination of motions corresponding to n = 2 and n = 3.

This approach is in agreement with the mathematics of equation (5.2). It is therefore possible to use a full-switching curve from that family and construct the maxpeak effect curves by analogy with the case n = 2 which is physically clearer. Fig. 5.2 presents such surves for n = 1.8. It can be seen that the maxpeak ratio, $\dot{x}_{xp}/\dot{x}_{fsp} = 1.44$ which is considerably larger than for n = 2 (maxpeak ratio = 1.33). Experimentally, n = 1.8 corresponds to F = 450 ma. (see Table 1, Chapter III and Fig. 3.2) for which $\dot{x}_{xp}/\dot{x}_{fsp} = 1.67$.

The argument, summarized, is that small values of F_{DN} corresponds to $n < 2$ and are associated with large maxpeak ratios. The assumption concerning the meaning of non-integer n leads, indeed, to larger maxpeak ratios as n decreases. The maxpeak ratio determined from the model is not as large, however, as experiment indicates.

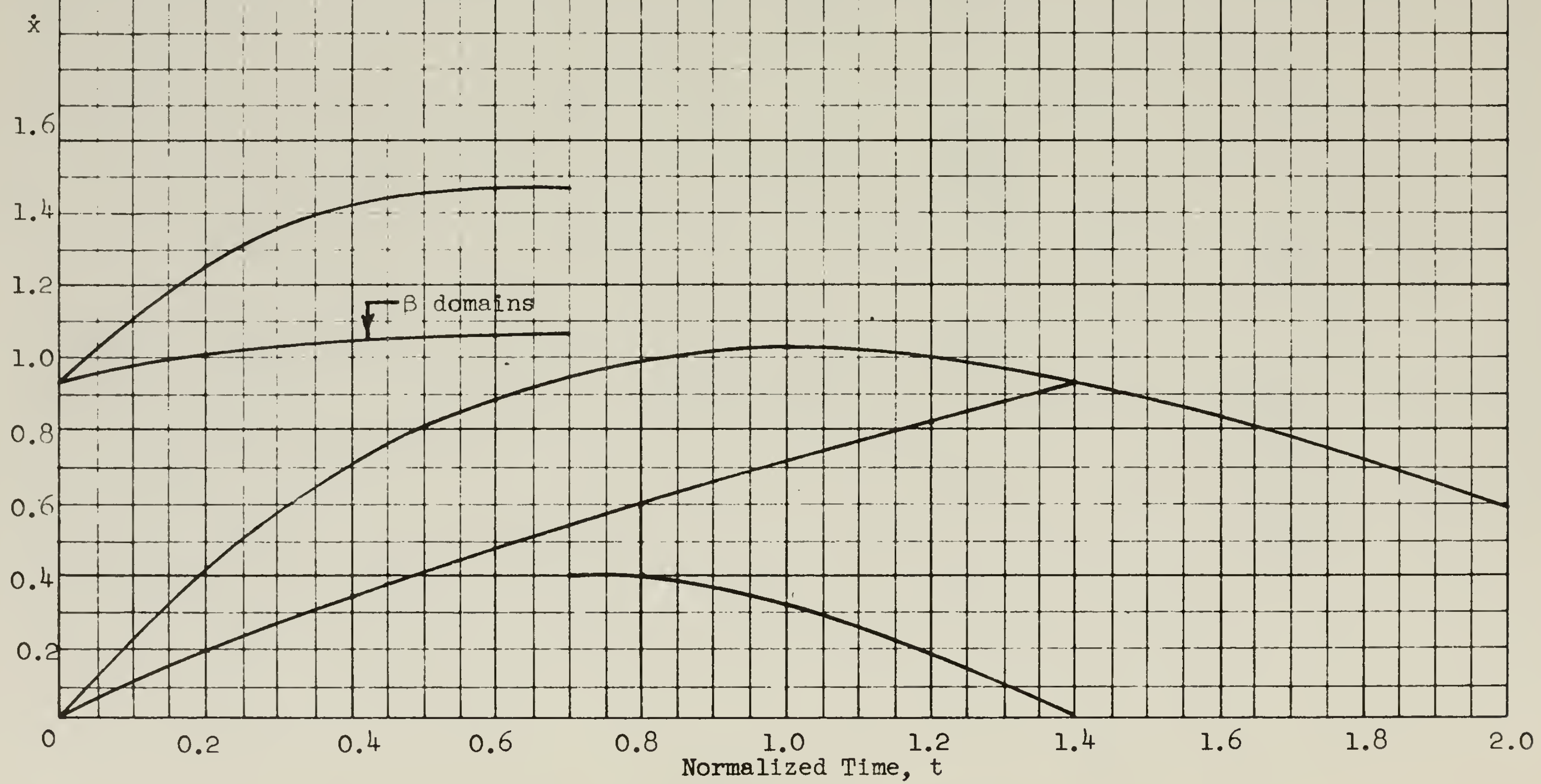

Figure 5.2 Maxpeak Curve for n = 1.8

The equations corresponding to this model are:

(Term 1)

$$\dot{x}_d = 2(n-1)\, K_d^n t_d^{n-1}\, e^{-(K_d t_d)^n} - \frac{K_d}{K_u}\, \dot{X}_u \left(\frac{t_d}{T_u}\right)^{n-1}$$

(Term 2)

$$+ \frac{K_d}{K_u}\, \dot{X}_u \left[\left\{\left(\frac{t_d}{T_u}\right)^{n-1} - \frac{t_d}{T_u}\right\} + \left\{\left(1 - \frac{t_d}{T_u}\right)^{n-1} - \left(1 - \frac{t_d}{T_u}\right)\right\}\right] \tag{5.3}$$

Term 1 applies for $0 \leq t_d \leq \frac{K_u T_u}{K_d}$.

Term 2 applies for $0 \leq t_d \leq \frac{K_u T_u}{2\, K_d}$.

CONCLUSION

1. General

The principal objective of the present investigation was the creation of a quantitative engineering model of a subclass of partial switching effects called, briefly, the "maxpeak effect".

Only scattered, uncoordinated experimental data has been available concerning partial switching effects in square-loop ferrites.[1] The present effort is believed to be the first attempt to reduce any partial switching effect to a quantitative engineering model.

In the pursuit of the primary goal of the investigation, some auxiliary results were obtained which are, perhaps, of interest. These are considered under the headings "Full Switching" and "Velocity Distribution".

2. Full Switching

The models of flux reversal by domain-wall motion as formulated by Haynes (1958) and Lindsey (1959) have been used as the starting point. These were generalized into a family of equations which has the desirable property that the curvature of the $1/\tau_s$ vs. F curve, which had been experimentally found, can be duplicated by adjustment of the generalizing parameter, n. It was shown that the value of n which fits a given experimental full switching curve can be conveniently calculated from the quantity, $\dot{x}_p t_p$, which is found to be independent of H, H_o, and S_w.

Since n can then be quite simply and unambiguously derived from experimental data, a distinction between the results of Haynes and of Lindsey can be made. No clear distinction had previously been demonstrated because

---

[1] Smith's (1960) collection of data is a notable exception.

all comparisons were dependent on the assignment of the parameters H_o and S_w. Thus, by normalization of the switching curves given by the two formulations, all practical distinction between them could be obliterated. By the new method of comparison, it is shown that Lindsey's model ($n = 2$) corresponds more closely to experiment in the region $H_o < H \leq 3H_o$.

An interesting aspect of the general family of switching equations is that the question of the physical interpretation (if any) of non-integer values of n arises. By analogy with the meaning of $n = 2$ and 3 from Lindsey's and Haynes' models respectively, it is proposed that the (non-zero) curvature of the reciprocal switching time curve may be due to changes in the average domain shape as a function of driving field.

This family of switching equations has the additional property that all usual definitions of switching time are related by an easily computed constant.

3. Maxpeak Effect Model for Limited Range of F_{DN}

The construction of a model of the maxpeak effect has been considered. The only strict invariant in the maxpeak effect was found to be the flux level at which maxpeak occurs. It was argued that the maxpeak effect is predominately a property of the magnetic material itself rather than the shape of the specimen since a thin-walled core, examined by Smith (1960), has a response nearly identical to a thicker-walled core. A "basic model" is constructed by extension of the details of Lindsey's model of full switching. In particular, it is assumed that domain walls which are not annihilated during the UP drive (β domains) are forced to retrace their route during the DOWN drive, and that renucleation occurs at the center from which the wall originated.

It was demonstrated that the basic maxpeak model predicts the maxpeak amplitude ratio, $\dot{x}_{xp}/\dot{x}_{fsp}$, very accurately for values of F_{DN} (viz., about $2H_o$) for which Lindsey's equation ($n = 2$) is considered to hold. On the other hand, the shape of the maxpeak effect curves predicted by the basic model is poor due to a sharp fall of amplitude which occurs. This fall is traced directly to the assumption of Menyuk and Goodenough (1955) (and retained by Haynes and Lindsey) that the domain wall velocity for a given driving field is constant (see Section 4, Conclusion).

Therefore, a new model was proposed which incorporates a Gaussian distribution of domain wall velocity. The mean velocity is assumed to be the velocity which would apply in the Menyuk-Goodenough theory. A standard deviation of 0.2 of the mean time of collapse of β domains has been found to be reasonable.

The maxpeak model including velocity distribution predicts switching curves whose shape conforms satisfactorily to experimental results. The accuracy of the fit between two curves is measured by the average absolute value of the error in percentage of peak amplitude. On this basis, the error between the theoretical and experimental maxpeak curve is about 6.5%.

It was demonstrated that the introduction of a velocity distribution, as described above, into the full switching equations results in only negligible alteration (about 1% in the switching curve). Therefore, the full and partial switching models are consistent after the velocity distribution is introduced.

Two further points have been clarified concerning the significance of radial effects within the toroidal sample. First, the question of whether radial variation of the driving field can be the cause of the maxpeak effect has been investigated. In extensive calculations, (Section IV.6) a member of the family of full switching curves (either n = 2, 3 or 4) was assumed to hold for each annulus of core material. The chosen expression for flux reversal was then integrated over path length in the magnetic material (from inner to outer core circumference). It was found that no rational values of H_o and S_w could be assigned which were reasonably accurate for both the full and partial switching cases. It was concluded from this investigation that radial effects are extremely unlikely to be the sole cause of the maxpeak effect and that, in fact, they are likely to be of only minor significance.

Secondly, the possible equivalence of the radial variation of the drive field with the wall velocity distribution chosen for the maxpeak effect was examined. Such equivalence appeared to be unlikely since, as previously noted, Smith's maxpeak curves for a thin core (OD/ID = 1.2) are not visibly different from those of a thicker core (OD/ID = 1.68) used in the present experiments. It is more probable that the maxpeak effect arises from the material properties, one of which is a distribution of domain-wall velocities for a given driving field.

4. Maxpeak Effect Model for Wider Range of F_{DN}

The maxpeak effect model discussed to this point is applicable only in a limited range of F_{DN}. Some success at extension of the basic maxpeak model to a wider range of F_{DN} was achieved by considering the

implications of the curvature of the $1/\tau_s$ vs. F curve. This curvature corresponds to variations in n, which is, perhaps, related to the average domain shape (see Section II, Conclusion). Since the wall length, L, of an active domain changes according to t^{n-1} for the full switching models, it is assumed that $L \propto t^{n-1}$ for non-integer n. Thus, the model is at least mathematically consistent for full switching and for the maxpeak effect over wide ranges of F_{DN}.

An example was given for the case n = 1.8. It was found that the maxpeak ratio has the proper direction of change but it is not as large as experiment indicates. Nevertheless, the model is, perhaps, of practical interest and probably of some theoretical interest.

5. Velocity Distribution

It had been assumed in the Menyuk-Goodenough theory of flux reversal that the domain wall velocity for a given driving field is constant (in any particular specimen of material). Perhaps the most interesting auxiliary result of the present investigation is that this assumption is not legitimate.

The conclusion that a velocity distribution is necessary was reached by consideration of a partial switching model. It is to be expected that a partial switching model requires a more accurate representation of domain activity than does a full switching model, the latter being a special case of the former.

It was found that the basic maxpeak model predicts a large, deterministic fall of potential which was not experimentally observed. The source of this fall was clearly traceable, from the theoretical viewpoint, to the formerly cited constant-velocity assumption of Menyuk and Goodenough.

The possibility that the fall of potential was not experimentally observed because of smoothing by radial effects was considered. It was shown that such smoothing could not account for the observations. Additional support for this view was provided by comparison of a maxpeak curve which had been observed by Smith (1960) for a thin-walled core with present experiments on a thicker-walled core. Since the two maxpeak curves are extremely similar, it was concluded that radial effects are not responsible for any substantial smoothing.

Therefore, the smoothness of the maxpeak effect curves is due, it was argued, to a material property, namely, the distribution of domain wall velocity. A normal distribution having the mean wall velocity equal to the Menyuk-Goodenough value and a standard deviation of 0.2 of that velocity was assumed. This distribution was demonstrated to smooth the maxpeak effect curves in approximately the desired way. Furthermore, the introduction of this same distribution into the full switching model was shown to produce only negligible change in the predicted full-switching curve.

It is therefore concluded that strong evidence has been provided for the existence of a distribution of domain wall velocity.

6. Further Work

The maxpeak models which have been proposed are based on the assumed activity of the so-called β domains. It would therefore be of considerable interest to experimentally determine whether the type of wall motion hypothesized for these domains does, indeed, exist.

A clearer understanding of the domain activity corresponding to curvature of the inverse-switching-time curve would also be of interest. This information would be invaluable to the formulation of a better model of switching both in the full and partial switching cases.

APPENDIX I

EXPERIMENTAL METHOD

1. Drive Pulse Amplitude and Length

Pulses corresponding to F_{UP} and F_{DN} were produced by mercury-wetted-contact relay pulsers in order to insure rectangularity of the pulse waveforms. The RESET pulse, critical only in amplitude and duration, was generated by a transistor driver.

The coaxial cables used with the relay pulsers were calibrated by the most accurate available techniques. Four pieces of cable having length ratios of approximately 1:2:4:8 were cut from a single lot of RG-62/U cable. Lengths were measured with a steel tape.

The velocity of propagation of each cable was measured by applying a stable variable-frequency oscillator to one end, the other end being either open or short circuited. Using a voltmeter to detect the nulls and peaks of the input voltage and measuring the oscillator frequency by means of the heterodyne with a precision 100 kc/s crystal-controlled harmonic generator, the velocity of propagation for the various cables was determined.

The average characteristic impedance of each was calculated by use of the measured total capacitance and velocity of propagation.

An accurately measured non-inductive resistor served as the termination of the pulser output. The amplitude of the drive current produced by the relay pulser is then given by $I = \frac{V}{R_t + R_0}$ where

V is the voltage to which the cable is charged, measured with a four-decimal-digit digital voltmeter

R_t is the resistance of the terminating resistor and

R_0 is the average characteristic resistance of the coaxial cable.

The above measurements allowed the complete specification of the drive pulses in both amplitude and duration within the limitations of the following considerations.

Besides the obvious sources of possible inaccuracy (e.g., accuracy of the capacitance bridge), several other sources remain. These are:

(a) the droop of the drive pulse due to cable losses,

(b) the resistance of the relay contact,

(c) the effective shortening of the drive pulse due to the initial inductance of the core, the open wire passing through it, and the relay contact leads,

(d) the reverse field from the current induced into the other drive and sense wires which pass through the core aperture (no more than one flux linkage was used for any drive or sense winding),

(e) capacitive coupling of drive pulses to the sense winding.

The effect (e) can be minimized by placing the core at the ground end of the output drive wire. This effect is further minimized by single-turn windings. The remaining spurious coupling is of sufficiently short duration that observation with a high speed oscilloscope (Tektronix Type 585) allows unambiguous observation of the main switching waveform.

The effects of (d) can be estimated by removing or adding resistance across an extra linking wire. This inaccuracy is usually negligible. The shortening in (c) is estimated to be no greater than one millimicrosecond. With respect to (b), the d.c. resistance is negligible while the variation due to contact bounce can be minimized by adjusting the relay drive frequency so that mechanical resonances are avoided. The drive pulse droop, (a) is of some consequence, being about 1% per 100 mμs. for RG-62/U cable. The average amplitude of the pulse can be estimated and used.

The transistor pulser used for resetting delivers a pulse of 50 mμs. rise time, 15 μs. duration and amplitude of 3a. using 2 parallel type 2N1072 transistors in the output. The amplitude is approximately 2.5 times the maximum drive used in any other part of the cyclic driving operations.

2. Waveform Measurement

Measurements were made directly on the oscilloscope display of the voltage-time waveform of the switching core. The peak amplitude of the core output voltage signal was measured by shifting the waveform with a d.c. voltage equal to the signal amplitude. The d.c. voltage was then measured with a digital voltmeter. Using Tektronix Type 585 oscilloscope, which has a considerably sharper focus than usual, it can be demonstrated that the maximum error due to visual reading of the beam's vertical position can be held to within 0.2 mm. which corresponds to 2 mv. for the vertical gain normally used here (100 mv./cm.).

If, after shifting the d.c. level of the signal for measurement and repositioning the beam, the zero level fell outside the limits stated

above (due, for example, to drifting of the oscilloscope's vertical position during measurement), the measurement was rejected.

Various slowly varying parameters (e.g., tilt of the horizontal line, calibration of the digital voltmeter) were checked before and after each group of measurements. Temperature was continuously monitored, and, finally, most measurements were repeated on subsequent days.

Peaking times were measured from the beginning of the drive pulse which is quite unambiguously marked by the fast rise time (3.5 mμs.) of the Type 585 oscilloscope. Unfortunately, however, the broadness of the voltage peak results in poor accuracy (perhaps 10%) in this measurement even for relatively fast (and, therefore, narrow-peaked) signals. Horizontal calibration of the scope was made by reference to 10 or 20 mc/s. sine waves from an accurate, crystal clock.

The limited accuracy of this measurement must be allowed for when comparisons to calculated data are made.

3. Size Measurements

Outside and inside diameters of cores were measured by means of a micrometer-adjusted microscope at a magnification corresponding to one micron per division of the micrometer scale. The average of two measurements taken along perpendicular lines were used in various calculations.

The inner and outer circumference of the core used in the present work were 2.238 mm. and 3.77 mm., respectively.

4. Core Type Used

A Telemeter Magnetic Type 50T5 core was used for all measurements cited in the test. This is a standard MgMn memory core apparently similar to General Ceramics S4 material.

APPENDIX II

RADIAL EFFECT AND MISCELLANEOUS COMPUTATIONS

1. General

A number of experimental computations were performed with the aid of the ILLIAC during the course of the present investigation. The various programs employed, totaling over thirty in number, can be categorized as follows:

(1) Compute a table of $\dot{x}(t)$ and $x(t)$ for the general full switching equation.

(2) Compute optimum values of S_w and H_o (and, optionally, ϕ_s) for fitting of a full switching curve (with or without radial effects) to experimental data. The minimization procedure used was variously: steepest descent, Newton's method, or a nameless hybrid method.

(3) Compute a table of $\dot{x}_{UP}$ and $\dot{x}_{DN}$ as a function of t for given F_u, T_u, F_d, and n with or without radial effects.

(4) Compute $\dot{x}_{DN}$ as a function of t with $\dot{x}_{DN} = a\dot{x}_{n_1} + (1-a)\,\dot{x}_{n_2}$. That is, $\dot{x}_{DN}$ is the weighted sum of two of the general switching curves.

(5) Compute $\dot{x}$ with H_o or S_w as a specified function of x.

2. Radial Effects

Integration of the switching equations over radius (or magnetic path length) of the core was commonly performed in the following way. If some member of the family of switching equations (3.4) is assumed to describe the switching of a differential radial thickness of core material,

then the switching equation including radial effects is:

$$v = \phi_s \cdot \frac{2nt^{n-1}}{\ell_b - \ell_a} \int_{\ell_a}^{\ell_b} \left[\frac{1.60\dot{6}}{S_w}\left(\frac{F}{\ell} - H_o\right)\right]^n \exp\left\{-\left[\frac{1.60\dot{6}}{S_w}\left(\frac{F}{\ell} - H_o\right) t\right]^n\right\} d\ell \qquad \text{(A II.1)}$$

where ϕ_s is the remanent flux (webers)

t is the time (μsec.)

F is the drive mmf (amperes)

H_o is the "threshold field" (amp./meter)

S_w is the switching constant (amp.-μsec./meter)

and v is the emf (volts).

Consistent units are listed parenthetically. The quantity $\frac{1.60\dot{6}}{S_w}\left(\frac{F}{\ell} - H_o\right) = K$.

The constant, $1.60\dot{6}$, is not essential to the formula but is included for completeness. The constant was obtained, originally, from Haynes' equation where it acts as an adjustment for the definition of switching time.

Equation (A II.1) was integrated by Simpson's Rule with appropriate checks to insure that the number of integration steps was sufficient to produce the desired accuracy of the result.

3. Curve Fitting

Given experimental data from the voltage-time waveform of the oscilloscope, it is frequently desirable to fit the data to some family of equations. In the earlier phases of the present investigation, the following method was used.

A number (usually 6) of experimental sets of values $\{v_i, t_i, F_i\}$ were recorded. Starting with trial values of H_o and S_w, equation (A II.1) was solved for the various $\{t_i, F_i\}$ to obtain v_i^*. The quantity $Q = \sum_i (v_i - v_i^*)^2$ was minimized by adjustment of H_o and S_w (and, perhaps, ϕ_s). That is, a "least square" criterion of minimization was used.

The foregoing procedure has the disadvantage that (a) the computation may be lengthy and (b) small errors in the experimental data may strongly affect the results. To abrogate difficulty (b), it would be necessary to use a larger number of experimental points which, unfortunately, increases the computation time.

It is possible, after some experience, to estimate the values of H_o and S_w which correspond to some prescribed peak amplitude and peaking time at a given n. A simple analysis program is then used to verify the estimated values.

Generally, it appears from experience that the most economical method of curve fitting is by means of a large number of previously prepared graphs of the various quantities of interest.

4. Maxpeak Effect

An attempt not previously described, to simulate the maxpeak effect was by linear combinations of portions of full switching equations under time translation. The results of this investigation were negative. It is possible to understand this by the following argument.

Consider a full switching curve of the general family displaced by time τ as in Fig. A II.1. Assume that the portion of the curve for $t > 0$ is a maxpeak curve. Therefore, the area under the curve for $t > 0$

should be about 0.8 of the total area. Then, the following equations must hold.

(1) $$\dot{x}_{xp} = 2n\left(\frac{n-1}{n}\right)^{\left(\frac{n-1}{n}\right)} e^{-\left(\frac{n-1}{n}\right)} K_d$$ where DOWN drive is assumed

(2) $$t_p - \tau = t_{xp}$$

(3) $$K_d \tau = (-\ln 0.8)^{1/n}$$

(4) $$t_p = \left(\frac{n-1}{n}\right)^{1/n} K_d$$

The above relations are to be found in Section III.2.

Combining (2), and (4);

(5) $$\tau = \frac{\left(\frac{n-1}{n}\right)^{1/n}}{K_d} - t_{xp}$$

Combining (3), (4), and (5);

(6) $$\frac{1}{K_d} (-\ln 0.8)^{1/n} = \frac{\left(\frac{n-1}{n}\right)^{1/n}}{K_d} - t_{xp}$$

Rearranging and using K_d from (1);

(7) $$\dot{x}_{xp} t_{xp} = 2n\left(\frac{n-1}{n}\right)^{\left(\frac{n-1}{n}\right)} e^{-\left(\frac{n-1}{n}\right)} \left(\frac{n-1}{n}\right)^{1/n} - (-\ln 0.8)^{1/n}$$

Solution of (7) for various n gives the following results:

n	$\dot{x}_{xp} t_{xp}$
2	0.403
3	0.629
4	0.746
10	0.956
∞	1.000

Experimentally it is found that $\dot{x}_{xp} t_{xp}$ is typically 1.375. Therefore, it is not possible to simulate a maxpeak curve by means of a single member of the family of (3.4), however translated.

Similarly, it can be seen that any linear combination of similar curves would tend to yield a value of $\dot{x}_{xp} t_{xp}$ which is too small compared to experiment. This is, indeed, the difficulty which is observed in attempting to simulate the maxpeak effect by linear combinations of switching curves having different n and, also, by radial effects.

For both of these cases, however, it should be noted that each component of the total waveform is not subject to the restriction that 80% of its total area lie to the right of $t = 0$. Only the resultant "maxpeak curve" must be so restricted. Therefore, the above analysis does not strictly apply to the cases considered.

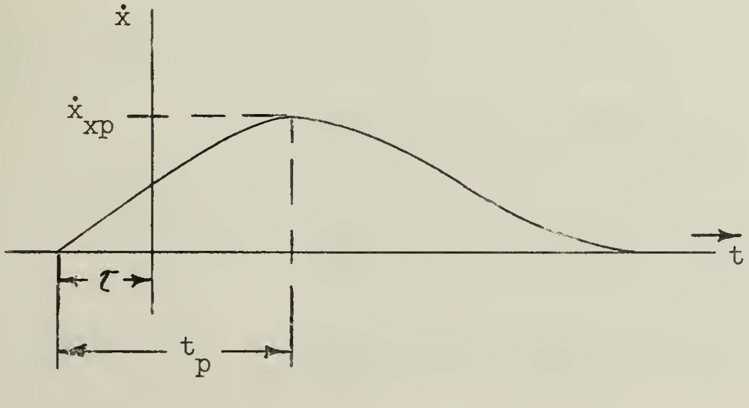

Figure A II.1

BIBLIOGRAPHY

Bardezh and Kobelef (1959) *Raschet Krevikh Pirimagnechevaniya Ferretovikh Sirridechnikof*, Institut Tochnoi Mechaniki e Vicheslete lnoi Techniki, Akademie Nauk, USSR. (Also published in *Magnetnie Elementi*, Moskva, 1960.)

Goodenough (1954) *A Theory of Domain Creation and Coercive Force in Polycrystalline Ferromagnetics*, Phys. Rev., vol. 95, no. 4, (August 1954).

Gyorgy (1957) *Rotational Model of Flux Reversal in Square-Loop Ferrites*, Jour. of Appl. Phys., vol. 28, no. 9, (September 1957).

Gyorgy (1958) *Rotational Model of Flux Reversal in Square-Loop Soft Ferromagnets*, Jour. of Appl. Phys., vol. 29, no. 3, (March, 1958).

Haynes (1958) *Model for Nonlinear Flux Reversal of Square-Loop Polycrystalline Magnetic Cores*, Jour. of Appl. Phys., vol. 29, no. 3, (March, 1958).

LFE (1960) *Research in Ferromagnetics*, Annual Report No. 570-A2, Computer Products Division, Laboratory for Electronics., Inc., Boston, Mass.

Lindsey (1959) *The Square-Loop Ferrite Core as a Circuit Element*, Proc. of the Inst. of Elec. Engrs., vol. 106, part C, no. 10, (September 1959).

Menyuk and Goodenough (1955) *Magnetic Materials for Digital Computer Components. I. A Theory of Flux Reversal in Polycrystalline Ferromagnetics*, Jour. of Appl. Phys., vol. 26, no. 1, (January 1955).

Shevel (1959) *Millimicrosecond Switching Properties of Ferrite Computer Elements*, Jour. of Appl. Phys., vol. 30S, no. 4, (April, 1959).

Smit and Wijn (1959) *Ferrites*, John Wiley and Sons, New York, (1959).

Smith (1960) *Flux Reversal in Ferrites*, Ph.D. Thesis, University of Toronto, Ontario, Canada, (April, 1960).

Tancrell and McMahon (1959) *Studies in Partial Switching of Ferrite Cores*, Technical Report No. 210, Lincoln Laboratory, Mass. Inst. of Tech., (September 1959).

Van Vleck (1956) *Fundamental Theory of Ferro- and Ferri-Magnetism*, Proc. of the IRE, vol. 44, no. 10, (October 1956).

BOUND BY
HNM

UNIVERSITY OF ILLINOIS-URBANA
510.84 IL6R v.1 C002 v.111-130(1961)
Some memory elements used in ILLIAC II /
3 0112 088404147